TITLE: COR27/28 Regulate the Evening Transcriptional Activity of the RVE8-LNK1/2 Circadian Complex

Maria L. Sorkin[a,b], Shin-Cheng Tzeng[a], Andrés Romanowski[c,1], Nikolai Kahle[d], Rebecca Bindbeutel[a], Andreas Hiltbrunner[d,e], Marcelo J. Yanovsky[c], Bradley S. Evans[a], and Dmitri A. Nusinow[a,2]

[a]Donald Danforth Plant Science Center, St. Louis, MO, USA.

[b]Division of Biology and Biomedical Sciences, Washington University in St. Louis, St. Louis, MO, USA

[c]Fundación Instituto Leloir, Instituto de Investigaciones Bioquímicas de Buenos Aires–Consejo Nacional de Investigaciones Científicas y Técnicas (CONICET), Buenos Aires, Argentina

[d]Institute of Biology II, Faculty of Biology, University of Freiburg, Freiburg, Germany

[e]Signalling Research Centres BIOSS and CIBSS, University of Freiburg, Freiburg, Germany

[1]current address: Department of Biology, Utrecht University, Utrecht, 3584 CH, The Netherlands

[2]to whom correspondence may be addressed. Email: meter@danforthcenter.org

Running title: Identification of the RVE8-LNK-COR27/28 regulatory complex

Abstract

The timing of many molecular and physiological processes in plants occurs at a specific time of day. These daily rhythms are driven by the circadian clock, a master timekeeper that uses daylength and temperature to maintain rhythms of approximately 24 hours in various clock-regulated phenotypes. The circadian MYB-like transcription factor REVEILLE 8 (RVE8) interacts with its transcriptional coactivators NIGHT LIGHT INDUCIBLE AND CLOCK REGULATED 1 (LNK1) and LNK2 to promote the expression of evening-phased clock genes and cold tolerance factors. While genetic approaches have commonly been used to discover new connections within the clock and between other pathways, here we use affinity purification coupled with mass spectrometry to discover time-of-day-specific protein interactors of the RVE8-LNK1/2 complex. Among the interactors of RVE8/LNK1/LNK2 were COLD REGULATED GENE 27 (COR27) and COR28, which were coprecipitated in an evening-specific manner. In addition to COR27/28, we found an enrichment of temperature-related interactors that led us to establish a novel role for LNK1/2 in temperature entrainment of the clock. We established that RVE8, LNK1, and either COR27 or COR28 form a tripartite complex in yeast and that the effect of this interaction *in planta* serves to antagonize transcriptional activation of RVE8 target genes through mediating RVE8 protein degradation in the evening. Together, these results illustrate how a proteomic approach identified time-of-day-specific protein interactions and a novel RVE8-LNK-COR protein complex that implicates a new regulatory mechanism for circadian and temperature signaling pathways.

Introduction

Daily and seasonal patterns in daylength and temperature cycles are two of the most dependable environmental cues an organism experiences. As such, lifeforms in every kingdom have evolved a mechanism to anticipate and synchronize their biology with the earth's predictable 24-hour and 365-day cycles (Ouyang et al., 1998; Rosbash, 2009; Edgar et al., 2012). This mechanism is called the circadian clock, which in plants consists of approximately 20-30 genes that participate in transcription-translation feedback loops to produce rhythms with a period of about 24 hours (Creux and Harmer, 2019). These core oscillator genes respond to the environment by producing a physiological response appropriate for a particular time of day or year (Webb et al., 2019). In plants, the clock regulates a variety of phenotypic outputs, including the transition

58 from vegetative to reproductive growth, biotic defense responses, and protection from abiotic
59 stressors such as extreme warm or cold temperature (Greenham and Mcclung, 2015).
60 Identification of circadian-associated genes has been critical in understanding the
61 generation of biological rhythms. Core oscillator components often exhibit rhythmic gene
62 expression with a period of ~24 hours and a set phase—or time of peak and trough expression. For
63 example, two of the first genes to be defined as core oscillator components in the model plant
64 *Arabidopsis thaliana* (Arabidopsis) are the morning-phased MYB-like transcription factors
65 *CIRCADIAN CLOCK ASSOCIATED 1* (*CCA1*) and *LATE ELONGATED HYPOCOTYL* (*LHY*)
66 (Schaffer et al., 1998; Wang and Tobin, 1998; Green and Tobin, 1999). These genes are highly
67 expressed at dawn and repress the expression of the afternoon- and evening-phased *PSEUDO*
68 *RESPONSE REGULATOR* genes *PRR1/ TIMING OF CAB EXPRESSION 1* (*TOC1*), *PRR5*, *PRR7*,
69 and *PRR9* (Alabadí et al., 2001; Farré et al., 2005; Kamioka et al., 2016). The *PRRs* reciprocally
70 repress *CCA1*/*LHY*, completing one of the negative feedback loops that define the clock. In the
71 evening, *EARLY FLOWERING 3* (*ELF3*), *ELF4*, and *LUX ARRHYTHMO* (*LUX*) interact in the
72 nucleus to form a tripartite protein complex called the evening complex, which represses *PRR9*,
73 *CCA1*/*LHY*, and other clock and growth-promoting factors (Dixon et al., 2011; Nusinow et al.,
74 2011; Chow et al., 2012; Herrero et al., 2012). As we discover new connections within and between
75 the clock, we enhance our understanding of this important system.
76 In this study, we used affinity purification coupled with mass spectrometry (APMS) to
77 identify protein-protein interactions associated with the REVEILLE 8 (RVE8)-NIGHT LIGHT-
78 INDUCIBLE AND CLOCK-REGULATED 1 (LNK1)/LNK2 circadian transcriptional complex.
79 The RVEs are an 8-member family of CCA1/LHY-like transcription factors of which some
80 members interact with the LNK proteins to coregulate target gene expression (Rawat et al., 2011;
81 Rugnone et al., 2013; Xie et al., 2014; Pérez-García et al., 2015; Gray et al., 2017). In the late
82 morning, the RVE8-LNK1/2 transcriptional complex activates the expression of evening-
83 expressed clock genes such as *TOC1* and *PRR5* via recruitment of the basal transcriptional
84 machinery to these and other *RVE8* target promoters (Xie et al., 2014; Ma et al., 2018). Conversely,
85 *LNK1/2* are also known to act as corepressors of other *RVE8* targets, such as the anthocyanin
86 structural gene *UDP-GLUCOSE:FLAVONOID 3-O-GLUCOSYLTRANSFERASE (UF3GT)*
87 (Pérez-García et al., 2015). Additionally, LNK1/2 interact with another transcription factor,
88 MYB3, as corepressors to inhibit the expression of the phenylpropanoid biosynthesis gene *C4H*

89 (Zhou et al., 2017). The mechanism behind the corepressive function of the LNKs and how they
90 switch between an activating and a repressive role is unknown.

91 LNK1/2 bind to RVE8 and MYB3 via two conserved arginine/asparagine-containing
92 motifs called R1/R2 located in the LNK C-terminus (Xie et al., 2014; Zhou et al., 2017).
93 Additionally, the Extra N-terminal Tail (ENT) domain present in LNK1/2 but not LNK3/4 is
94 required for their repressive activity with MYB3 (Zhou et al., 2017). The LNKs have no other
95 known functional protein domains apart from these regions. RVE8 and the other RVEs are
96 characterized by the presence of a LHY-/CCA1-LIKE (LCL) domain, which can directly bind the
97 LNKs, presumably at the C-terminus (de Leone et al., 2018; Ma et al., 2018). RVE8 target gene
98 promoters frequently contain the canonical *CCA1*/*LHY*-binding motif called the evening element
99 (EE) as well as G-box-like and morning element (ME)-like motifs (Hsu et al., 2013a).

100 In addition to regulating circadian rhythms, *RVE4*/8 regulate thermotolerance under both
101 high and low temperatures (Li et al., 2019; Kidokoro et al., 2021). After exposure to heat shock,
102 RVE4/8 upregulate the expression of *ETHYLENE RESPONSIVE FACTOR 53* (*ERF53*) and
103 *ERF54*, boosting the plant's heat shock tolerance (Li et al., 2019). In another study, the authors
104 found that *RVE4*/8 also appear to promote freezing tolerance via activation of *DEHYDRATION-*
105 *RESPONSIVE ELEMENT BINDING PROTEIN 1A* (*DREB1A*, also referred to as *C-REPEAT*
106 *BINDING FACTOR 3, CBF3*) when grown at 4°C (Kidokoro et al., 2021). A corresponding
107 association between temperature and the LNKs has not been well studied, although EC-mediated
108 induction of *LNK1* expression under warm nights suggests a role for the LNKs in temperature
109 responses (Mizuno et al., 2014).

110 Our proteomic approach presented here establishes novel protein interactions with the
111 RVE8-LNK1/2 transcriptional complex at ZT5 and ZT9. Although these clock bait proteins exhibit
112 peak mRNA expression in the early morning hours, we found that LNK1 and RVE8 interact with
113 more protein partners at the later ZT9 timepoint than at ZT5. Temperature response related GO
114 terms were significantly enriched among the coprecipitated proteins, prompting us to explore and
115 establish a role for LNK1/2 in temperature entrainment of the clock. Among the temperature-
116 related coprecipitated proteins were COLD REGULATED GENE 27 (COR27) and COR28, which
117 only coprecipitated with RVE8/LNK1/LNK2 at ZT9. Furthermore, we found that the CORs
118 interact with RVE8 and LNK1 in a tripartite complex in a yeast 3-hybrid system. By performing
119 APMS using 35S::YFP-COR27 and 35S::GFP-COR28, we validated the interaction with LNK1,

120 LNK2, and RVE8, and identified additional novel interactions between the CORs and RVE5,
121 RVE6, and several light signaling proteins. Further investigation into the role of the RVE8-
122 LNK1/2-COR27/28 interaction suggested that the CORs antagonize activation of RVE8 target
123 genes via regulation of RVE8 protein stability in the evening. Thus, by taking a proteomic
124 approach to study a core circadian transcriptional complex, we identified a novel, evening-phased
125 RVE8-LNK-COR protein complex that presents a new regulatory mechanism for circadian and
126 temperature signaling pathways.
127

128 **Results**

129 **Characterization of affinity-tagged lines**

130 To identify new interactions with known clock proteins, we created endogenous promoter-
131 driven, 3x-FLAG-6x-His C-terminal (HFC) affinity-tagged versions of RVE8, LNK1, and LNK2.
132 RVE8-HFC was transformed into the *rve8-1 CCR2::LUC* mutant background while LNK1-HFC
133 and LNK2-HFC were introduced into *lnk1/2/3/4* quadruple mutant (*lnkQ)* (de Leone et al., 2018)
134 *CCA1::LUC.* By transforming our tagged LNKs into the *lnkQ* background, we could eliminate co-
135 precipitating interactors that could be formed through a complex between our tagged LNKs and
136 the endogenous LNKs. To ensure the tagged versions of our proteins of interest functioned
137 similarly to their native counterparts, we selected T3 homozygous lines that rescued the long
138 period mutant phenotype of *rve8-1* or *lnkQ* mutants (Rawat et al., 2011; Xie et al., 2014) (**Fig. 1A-**
139 **C**). LNK1-HFC/LNK2-HFC did not fully restore the circadian period back to wild-type levels, but
140 the lengthened period is consistent with the absence of the other three LNKs after the introduction
141 of the tagged LNK into the *lnkQ* quadruple mutant (Xie et al., 2014; de Leone et al., 2018). We
142 also determined that the HFC-tagged proteins exhibit rhythmic protein abundance patterns under
143 12 hr light: 12 hr dark (LD) conditions, as would be expected for these proteins (**Fig. 1D-G**). While
144 mRNA expression for *RVE8*, *LNK1*, and *LNK2* peaks at ZT1, ZT5, and ZT2, respectively, peak
145 protein abundance occurred at ZT6, ZT9, and ZT6—about 4-5 hours after peak mRNA expression
146 (Mockler et al., 2007) (**Fig. 1D-G, Fig. S1**). This lag in protein abundance after transcription is
147 consistent with previously reported data showing a peak in RVE8-HA abundance three to six hours
148 after dawn (Rawat et al., 2011). These experiments demonstrate that our affinity-tagged clock
149 proteins behaved similarly to the native protein and are functional, making them ideal tools for
150 capturing relevant protein interactions.

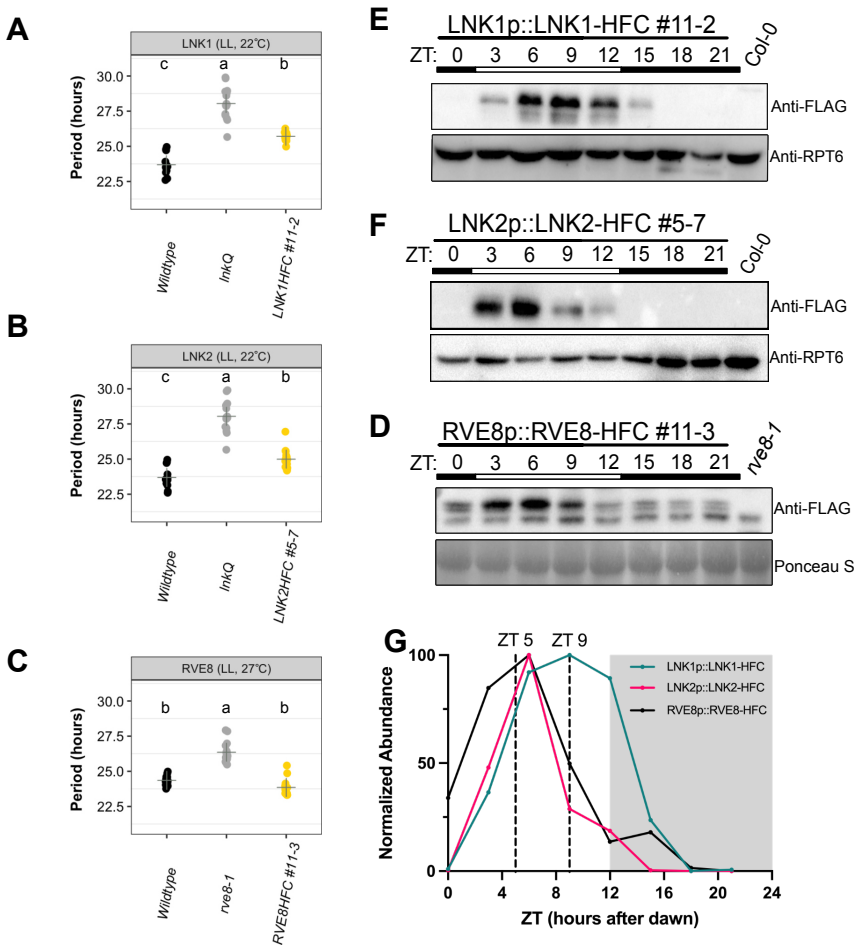

Figure 1 Characterization of affinity-tagged lines used for APMS (A-C) Circadian luciferase reporter period analysis of selected T3 homozygous lines expressing (A) LNK1-HFC, (B) LNK2-HFC, or (C) RVE8-HFC in their respective mutant backgrounds (*rve8-1* or *lnkQ*). Each point represents the circadian period of an individual plant and the + symbol shows the average period for that genotype. Letters correspond to significantly different periods as determined by ANOVA with a Tukey's post-hoc test. LNK1 and LNK2 luciferase assays were performed together and include the same wildtype and *lnkQ* data. Environmental conditions during imaging are included at the top of the plot (LL = constant light). (D-F) Time course Western blots showing cyclic protein abundance patterns of 10-day-old affinity tagged lines under 12 hr light: 12 hr dark 22 °C conditions. Affinity tagged lines are detected with anti-FLAG antibody. RPT5 or Ponceau S staining was used to show loading. Col-0 CCA1::LUC (Col-0) or *rve8-1* CCR2::LUC (*rve8-1*) were used as negative controls. White and black bars indicate lights-on and lights-off, respectively (D) 24-hour protein expression patterns of affinity tagged lines normalized to Ponceau S or RPT5 quantified by densitometry of Western blots shown in D-F. Vertical dotted lines indicate time of tissue collection for APMS. White and grey shading indicates lights-on and lights-off, respectively. Western blots and luciferase reporter assays were repeated at least 2 times. ZT= Zeitgeber Time.

151

152

153 **Affinity purification-mass spectrometry (APMS) identifies novel time-of-day-specific**
154 **interacting partners for RVE8, LNK1, and LNK2**

155 We selected two timepoints for APMS based on the protein abundance patterns for RVE8-
156 HFC, LNK1-HFC, and LNK2-HFC **(Fig. 1G**). RVE8-HFC and LNK2-HFC exhibited the highest
157 protein abundance between ZT3 and ZT6, while LNK1-HFC protein was highest between ZT6
158 and ZT9. Considering this, we chose to examine protein-protein interactions at ZT5 and ZT9.

159 We identified a total of 392 proteins that coprecipitated with either RVE8-HFC, LNK1-
160 HFC, or LNK2-HFC at ZT5 or ZT9 but did not coprecipitate in our GFP-HFC nor Col-0 negative
161 controls (**Fig. 2A, Dataset S1**). Consistent with the time of peak LNK1-HFC and LNK2-HFC
162 protein abundance (ZT9 and ZT5, respectively; **Fig. 1G**), we saw higher total spectra mapping to
163 LNK1-HFC at ZT9 (621) and LNK2-HFC at ZT5 (497) compared to the other timepoint (**Tables**
164 **1 and 2**). Similarly, the number of coprecipitated proteins was greatest at ZT9 for LNK1-HFC and
165 at ZT5 for LNK2-HFC (**Fig. 2B-C, Dataset S1**). Total spectra mapping to the bait protein RVE8-
166 HFC were similar between the two timepoints (**Tables 1 and 2**). Despite the similarity in RVE8-
167 HFC total spectra between timepoints, we precipitated more ZT9-specific interactors than ZT5-
168 specific interactors with RVE8-HFC (**Fig. 2D**). Overall, we identified more RVE8/LNK1/LNK2-
169 binding partners at ZT9 (364) versus the earlier timepoint of ZT5 (281) (**Fig. 2A**) and found that
170 111 out of 392 (28.3%) total proteins coprecipitated were ZT9-specific; these proteins were not
171 coprecipitated in any APMS experiment performed at ZT5. In summary, the enrichment of
172 coprecipitated proteins at ZT9 suggests an important post-translational role for the RVE8-LNK1/2
173 complex in the evening.

174 We used gene ontology (GO) analysis to categorize coprecipitated proteins at ZT5, ZT9,
175 and ZT5/9 (**Fig. 2A**). Proteins coprecipitated at ZT5 only were mostly assigned GO biological
176 process terms associated with homeostasis and general metabolism while proteins found at ZT9
177 only or ZT5/ZT9 fell into relevant categories such as 'regulation of circadian rhythm', 'response
178 to light stimulus', and 'photoperiodism' (**Fig. 2A**). We also noted that GO terms associated with
179 temperature response were enriched in our interactor dataset ('response to cold', 'response to
180 temperature stimulus', and 'response to heat') (**Fig. 2A**). This analysis suggested that we identified
181 biologically relevant interacting partners involved in circadian rhythms in our APMS experiments
182 and that there is an enrichment of temperature-related factors among these interactors. We also
183 cross-referenced our lists of coprecipitated proteins with known cycling genes (Romanowski et

184 al., 2020) and found that 71.0% of ZT5 and 71.1% of ZT9 proteins exhibited cyclic mRNA
185 expression (**Dataset S1**), demonstrating that our bait circadian clock proteins mostly interacted
186 with proteins whose expression also cycles.

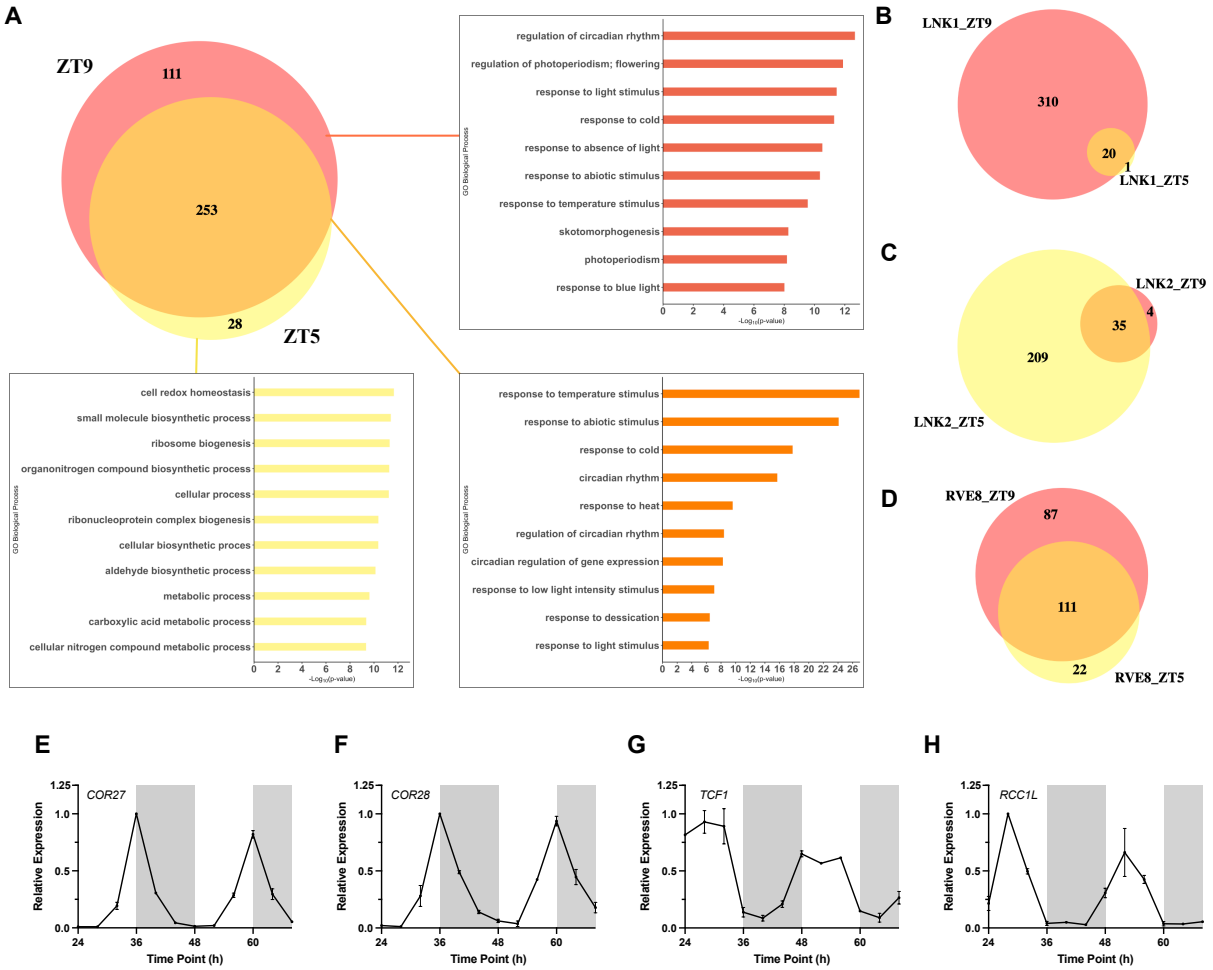

Figure 2 Analysis of proteins coprecipitated with RVE8/LNK1/LNK2-HFC by time-of-day affinity purification-mass spectrometry (A) Venn diagram showing number of proteins coprecipitated with RVE8/LNK1/LNK2 at ZT5, ZT9, or at both timepoints. Corresponding bar charts show enriched GO biological process terms with -Log10$_{(p\text{-value})}$. (B-D) Venn diagrams of coprecipitated proteins at ZT5 and ZT9 separated by bait protein (B, LNK1-HFC, C, LNK2-HFC, or D, RVE8-HFC). (E-H) mRNA expression profiles in constant light of four cold-response proteins identified as RVE8/LNK1/LNK2 interactors. RNA-seq data for E-H taken from Romanowski et al. (2020) *The Plant Journal*. ZT= Zeitgeber Time

187 Among the top interactors for LNK1-HFC, LNK2-HFC, and RVE8-HFC were four cold-
188 response proteins: COLD REGULATED GENE 27 (COR27), COR28, and two regulator of
189 chromosome condensation family proteins, TOLERANT TO CHILLING/FREEZING 1 (TCF1),
190 and a homolog of TCF1 that we named REGULATOR OF CHROMOSOME CONDENSATION
191 1-LIKE (*RCC1L*, AT3G53830) (**Tables 1-2**). We characterized these as high-priority interactors
192 based on their subcellular localization prediction and mRNA expression patterns; all four proteins

193 are predicted to be nuclear localized according to the SUBACon subcellular localization consensus
194 algorithm (Hooper et al., 2014), which stands in agreement with being interactors of the nuclear-
195 localized RVE8/LNK1/LNK2 proteins; additionally, the mRNA expression for these genes is
196 rhythmic under constant light conditions, suggesting circadian regulation of their expression (**Fig.**
197 **2E-H**). TCF1 and RCC1L were coprecipitated with RVE8/LNK1/LNK2 at both ZT5 and ZT9
198 while COR27/28 were ZT9-specific interactors **(Tables 1-2**).
199
200 *TCF1* and *RCC1L* are homologs of the regulator of chromosome condensation (RCC)
201 family protein, RCC1 (Ji et al., 2015) and share 49.7% identity in an amino acid alignment (**Fig.**
202 **S2**). RCC1 is a highly conserved guanine nucleotide exchange factor (GEF) for the GTP-binding
203 protein RAN and is involved in nucleocytoplasmic export along with regulation of the cell cycle
204 via chromosome condensation during mitosis (Ren et al., 2020). While there are no previous
205 publications characterizing *RCC1L,* its sister gene *TCF1* is a known negative regulator of cold
206 tolerance in Arabidopsis via the lignin biosynthesis pathway (Ji et al., 2015). *RCC1L* expression
207 is downregulated upon cold treatment (**Table S1**), but no formal studies have been made into its
208 role in cold tolerance nor chromatin biology.
209 COR27/28 have no known protein domains and are repressors of genes involved in cold
210 tolerance, circadian rhythms and photomorphogenesis (Li et al., 2016; Wang et al., 2017; Kahle et
211 al., 2020; Li et al., 2020; Zhu et al., 2020). Notably, COR27/28 repress the same clock and cold
212 tolerance genes that are activated by RVE8; *PRR5*, *TOC1*, and *DREB1A* are repressed by the CORs
213 and activated by RVE8 (Rawat et al., 2011; Kidokoro et al., 2021). Null or knock-down mutants
214 of *cor27*/*cor28* exhibit a long period mutant phenotype, similar to that observed for *lnk* and *rve8*
215 mutants (Rawat et al., 2011; Rugnone et al., 2013; Li et al., 2016). As the CORs do not contain a
216 known DNA-binding domain, it is not understood how, mechanistically, these factors alter
217 transcription.
218 Among the 111 evening-specific interactors were COR27, COR28, CONSTITUTIVELY
219 PHOTOMORPHOGENIC 1 (COP1), and SUPPRESSOR OF PHYA-105 (SPA1) (**Table 2**).
220 COP1 and SPA1 were RVE8-HFC-specific interactors while COR27/28 coprecipitated at ZT9
221 with LNK1/LNK2/RVE8-HFC. We hypothesized that this time-of-day-specific coprecipitation
222 could be explained by the relative abundance of these proteins at ZT5 versus ZT9 due to diurnal
223 changes in gene expression over the course of the day. To investigate this hypothesis, we overlayed

224 the LD mRNA expression patterns of these ZT9-specific interactors on top of the protein
225 abundance levels of RVE8-HFC, LNK1-HFC, and LNK2-HFC that were determined by time
226 course Western blots shown in **Figure 1D-F** (**Fig. S3**). There is very little overlap in expression
227 between the *CORs* and *RVE8/LNK1/LNK2* at ZT5 (**Fig. S3)**, indicating that COR27/28 may have
228 only coprecipitated at ZT9 due to increased expression at that timepoint. In contrast, there was not
229 a clear time-of-day distinction in expression overlap between COP1/SPA1 and the clock bait
230 proteins, suggesting the ZT9-specific interaction between COP1/SPA1 and RVE8-HFC is possibly
231 due to a factor other than expression level, such as recruitment through other proteins (such as
232 COR27 or COR28) (**Fig. S3**).
233
234 **COR27 and COR28 interact with circadian and light signaling proteins**
235 To better understand the role of COR27/28 at the protein level, we performed APMS using
236 35S::YFP-COR27 and 35S::GFP-COR28 lines (Li et al., 2016) collected at ZT9. Through this
237 experiment, we validated the interactions between the CORs and RVE8/LNK1/LNK2 and
238 additionally coprecipitated RVE5 and RVE6, further supporting the connection between
239 COR27/28 and the RVE/LNK proteins (**Table 3, Dataset S1**). Previous studies have shown an
240 interaction between COR27/28 and PHYTOCHROME B (PHYB), COP1, and SPA1 (Kahle et al.,
241 2020; Li et al., 2020; Zhu et al., 2020). Our affinity purification captured these known interactions
242 and additionally identified PHYD and SPA2/3/4, supporting the previously demonstrated role for
243 the CORs in photomorphogenesis (**Table 3**) (Kahle et al., 2020; Li et al., 2020; Zhu et al., 2020).
244 TCF1, one of the cold-tolerance proteins (Ji et al., 2015) to coprecipitate with RVE8/LNK1/LNK2,
245 was also captured with COR27 (**Table 3**), which further implicates the CORs in freezing tolerance.
246 In total, we identified 268 proteins that coprecipitated with YFP-COR27 or GFP-COR28 (**Dataset**
247 **S1**). Of these, we found 58.9% exhibited circadian-regulated mRNA (Romanowski et al., 2020)
248 (**Dataset S1**). Together, the COR27/28 APMS provides strong evidence that these proteins are
249 important factors in circadian and light signaling networks.
250
251 **RVE8, LNK1, and COR27/28 form a protein complex**
252 We used a yeast 2-hybrid system to validate the interactions identified in our APMS
253 between RVE8/LNK1/LNK2 with COR27/28. Surprisingly, we did not see a positive interaction
254 between these components when using a binary yeast 2-hybrid (**Fig. S4)**. Since APMS can identify

255 both direct and indirect protein-protein interactions, we hypothesized that RVE8-LNK1/2-
256 COR27/28 could be forming a protein complex where the CORs can only bind when both RVE8
257 and LNK1 are present. To test this, we used a yeast 3-hybrid system in which a linker protein is
258 expressed in addition to the bait and prey proteins. We used N- and C-terminal truncations of
259 LNK1 since full-length LNK1 autoactivates in yeast, as has been shown previously and here **(Fig.**
260 **S5**) (Xie et al., 2014). Using this method, we found that yeast expressing RVE8, the C-terminus
261 of LNK1, and COR27 or COR28 were able to grow on selective media in a higher order complex
262 (**Fig. 3**). Yeast strains where COR27 or COR28 was paired with either LNK1 or RVE8 alone were
263 unable to grow on selective media, indicating that indeed all three components must be present for
264 the CORs to bind (**Fig. 3, S4**). We also confirmed that RVE8 interacts with the C-terminus of
265 LNK1 (**Fig. S4**), in agreement with previous studies (Xie et al., 2014). In combination with our
266 time-of-day APMS, these results show the CORs interact with RVE8/LNK1 in a complex that is
267 present at ZT9.

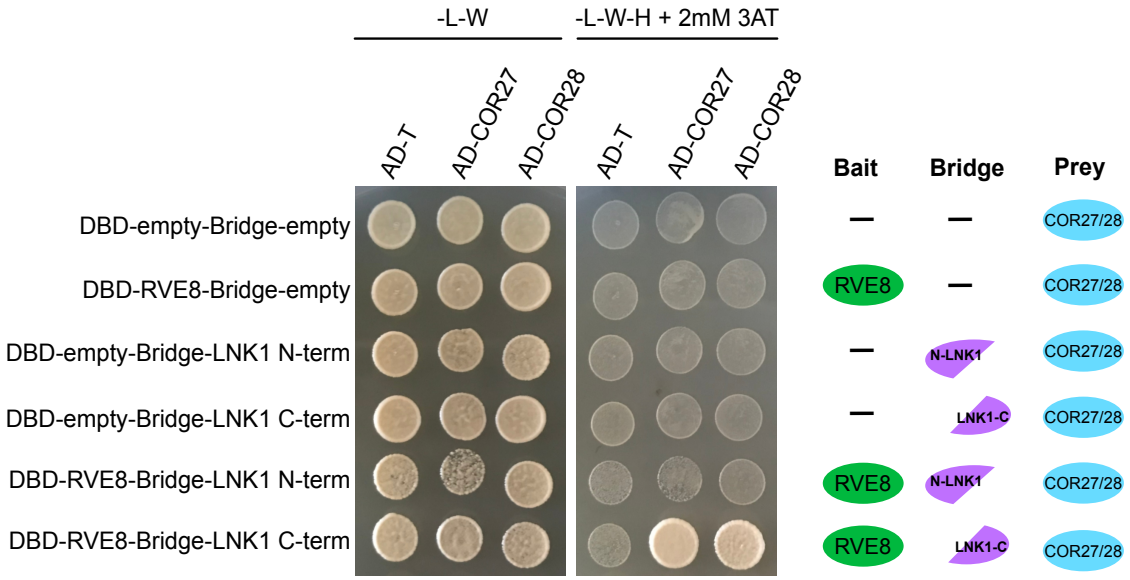

Figure 3 COR27/28 interact with RVE8/LNK1 in a yeast 3-hybrid system Yeast strains Y2H Gold or Y187 expressing pBridge (GAL4-DBD and a Bridge protein) or pGADT7 (GAL4-AD), respectively, were mated and plated onto selective media. Successful matings can grow on -Leucine/-Tryptophan media (-L-W) while positive interactors can grow on -Leucine/-Tryptophan/-Histidine + 2mM 3-amino-1,2,4-triazole (3AT) (-L-W-H + 2mM 3AT). A graphical depiction of different combinations is shown to the right. AD-T (large T-antigen protein) is a negative control for prey interactions. Experiment was repeated at least twice.

268 **COR27/28 alter diurnal RVE8 protein abundance patterns and antagonize activation of the**
269 **RVE8 target gene *TOC1***

270 We next sought to determine the biological relevance of the RVE8-LNK1/2-COR27/28
271 interaction. COR27/28 are post-translationally regulated via degradation by 26S proteasome
272 (Kahle et al., 2020; Li et al., 2020; Zhu et al., 2020). As COR27/28 were identified as ZT9-specific
273 RVE8-HFC interactors (**Table 2**), we hypothesized that COR27/28 target the RVE8-LNK
274 complex for degradation in the evening, thus blocking expression of RVE8 target genes late in the
275 day. To determine if RVE8-HFC abundance patterns are driven by a post-translational mechanism,
276 we examined protein abundance of RVE8-HFC in seedlings treated with either the 26S proteasome
277 inhibitor bortezomib (bortz) or DMSO (mock). The mock treated seedlings showed the typical
278 pattern for RVE8-HFC protein abundance (**Fig. 1F**) with decreasing RVE8-HFC from ZT6 to
279 ZT15 (**Fig. S6**). Treatment with bortz led to increased RVE8-HFC accumulation during this time
280 frame, indicating 26S-proteasome degradation is involved in the observed decrease of RVE8-HFC
281 from ZT6 to ZT15 (**Fig. S6**).

282 Next, we tested if COR27 and COR28 regulate RVE8 protein abundance by examining
283 cyclic protein abundance in RVE8p::RVE8-HFC versus RVE8p::RVE8-HFC in *cor27-2 cor28-2*.
284 While RVE8-HFC abundance in the wild-type background exhibits rhythmic protein abundance
285 with peak protein levels at ZT6, RVE8-HFC abundance is significantly higher in the *cor27-2*
286 *cor28-2* background during the evening and nighttime hours (**Fig. 4A-C**). This result is consistent
287 with the hypothesis that in the absence of COR27/28, RVE8-HFC should be stabilized specifically
288 in the evening—when it would normally be degraded through its interaction with the CORs. As
289 the circadian rhythm of *RVE8* mRNA expression under LD cycles was shown to be unchanged in
290 the *cor27-2 cor28-2* background (Wang et al., 2017), our results indicate that COR27/28 regulate
291 RVE8-HFC protein abundance at the post-translational level.

292 We then tested the effect of the CORs on RVE8/LNK1 transcriptional activity using a
293 transactivation assay in *Nicotiana benthamiana* (**Fig. 4D**). RVE8 binds to the evening element cis-
294 regulatory motif in the *TOC1* promoter to activate its expression (Rawat et al., 2011). When LNK1
295 and RVE8 were transiently expressed together in *N. benthamiana* along with a *TOC1* promoter-
296 driven luciferase reporter, we observed activation of the reporter, as expected (**Fig. 4D**). When
297 COR27 or COR28 was added to the inoculation cocktail, activation of the reporter was reduced,
298 indicating that the CORs antagonize RVE8/LNK1 transcriptional activity *in vivo* (**Fig 4D**). Taken

299 together, our results indicate that the RVE8-COR27/28-LNK1/2 interaction serves to block
300 activation of RVE8 target genes via degradation of RVE8 in the evening.

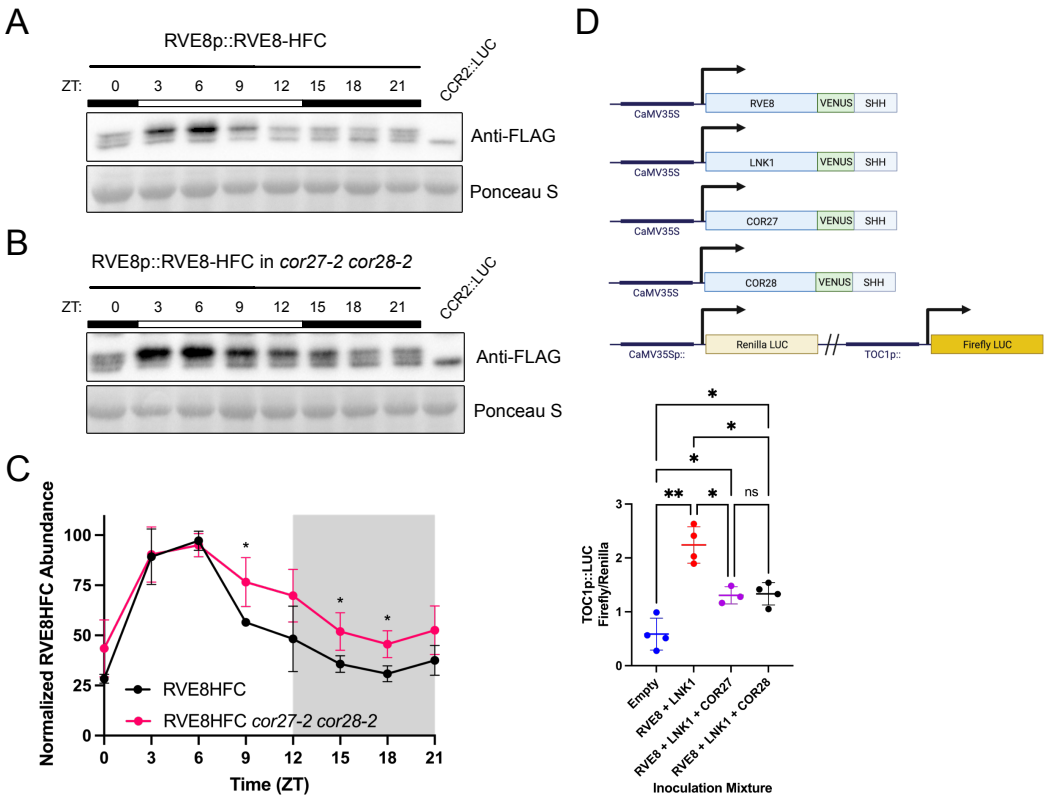

Figure 4 COR27/28 alter RVE8-HFC protein abundance patterns and inhibit RVE8/LNK1-mediated activation of *TOC1* (A-B) 24-hour protein expression patterns of RVE8-HFC in wild type (A) or *cor27-2 cor28-2* (B) backgrounds analyzed by Western blot. Tissue was collected every 3 hours from 12-day-old plants grown under 12 hr light: 12 hr dark 22 °C conditions. Anti-FLAG antibody was used to detect RVE8-HFC and Ponceau S staining was used to show loading. White and black bars indicate lights-on and lights-off, respectively. Col-0 CCR2::LUC was used as the negative control. (C) Densitometry quantification of (A) and (B) RVE8-HFC 24-hour abundance normalized to Ponceau S in wild type and *cor27-2 cor28-2* backgrounds. Points represent the average normalized RVE8-HFC abundance from 3 (WT) or 4 (*cor27-2 cor28-2*) independent bioreps. Asterisks indicate significant differences between genotypes based on Welch's t-test (* $p < 0.05$). Error bars = SD. (D) Dual luciferase assay in 3–4-week-old *Nicotiana benthamiana*. Schematic of expression constructs infiltrated are shown at the top (SHH = 2X-StrepII-HA-His_6 tag). Luminescence from a dual firefly/renilla luciferase reporter was measured after coinfection with 35S::RVE8-VENUS-SHH, 35S::LNK1-VENUS-SHH, 35S::COR27-VENUS-SHH, or 35S::COR28-VENUS-SHH. Luminescence was normalized to constitutively expressed renilla luciferase luminescence to control for infection efficiency. Points represent the normalized luminescence from 3-4 independent experiments with N=12. Mean normalized luminescence is indicated by the crosshair symbol and error bars = SD. Asterisks indicate significant differences by unpaired t-test with Welch correction (ns= not significant, * $p < 0.05$, ** $p < 0.01$). ZT= Zeitgeber Time. Empty = reporter alone.

301 **The RVEs are important for cold temperature induction of COR27/28**

302 *COR27/28* contain evening elements in their promoters that are important for their cold
303 induction and could be targets of RVE8 transcriptional regulation (Mikkelsen and Thomashow,
304 2009; Wang et al., 2017). Additionally, *COR27/28* are significantly upregulated in an inducible
305 RVE8:GR line according to a previously published RNA-seq dataset (Hsu et al., 2013b). Both
306 COR27/28 and RVE4/8 regulate cold tolerance in Arabidopsis; *COR27/28* expression is induced
307 by cold temperature (16 °C and 4 °C) within 3 hours and the *cor27-1 cor28-2* loss-of-function
308 mutant shows increased freezing tolerance, suggesting these genes are negative regulators of the
309 plant's response to freezing temperatures (Li et al., 2016). In contrast, RVE4/8 are activators of
310 cold tolerance (Kidokoro et al., 2021). Upon cold treatment (4°C for 3 hours), RVE4/8 localize to
311 the nucleus and upregulate *DREB1A* to promote freezing tolerance (Kidokoro et al., 2021).

312 To determine if the RVE transcription factors are regulators of *COR27/28* cold-induction,
313 we examined *COR27/28* expression at 22 °C and 4 °C in Col-0, *rve8-1, rve34568,* and *lnkQ*
314 mutants. We found that *COR27/28* cold-induction was greatly attenuated in *rve34568* and *lnkQ*
315 mutants, consistent with the *CORs* being targets of the RVE-LNK transcriptional complex (**Fig.**
316 **S7A-B)**. The absence of an effect in the *rve8-1* single mutant suggests there is redundancy among
317 the *RVE* family in the regulation of *COR27/28*. Indeed, we found that the LNKs coprecipitated
318 RVE3/4/5/6/8 in our APMS (**Tables 1 and 2**), suggesting multiple RVE/LNK complexes could
319 influence the regulation of the *CORs*. Interestingly, we saw little effect of RVEs/LNKs on
320 *COR27/28* expression at 22 °C at ZT12 (**Fig. S7C-D**), suggesting these clock factors only have an
321 effect under cold stress or that there may be a greater effect on expression at 22 °C at a different
322 time of day.

323

324 **LNK1 and LNK2 are important for temperature entrainment of the clock**

325 The enrichment of temperature response GO terms among the list of coprecipitated proteins
326 in our APMS (**Fig. 2A**), as well as the existing evidence linking RVE8 to temperature regulation
327 (Blair et al., 2019; Kidokoro et al., 2021) prompted us to investigate whether *LNK1/2* are important
328 for temperature input to the clock. While light is the primary entrainment cue for the plant clock,
329 daily temperature cycles are known to be another major environmental input cue (Devlin and Kay,
330 2001; Salomé and Robertson Mcclung, 2005; Avello et al., 2019). To examine temperature
331 entrainment, we examined rhythms from a CCA1::LUC reporter in wild type and *lnk1-1, lnk2-4,*

332 and *lnk1-1 lnk2-4* mutant plants that were first grown under constant light and then transferred into
333 a temperature entrainment condition. Under constant light, the *lnk* mutants exhibited their
334 canonical long period mutant phenotype (Rugnone et al., 2013) (**Fig. 5**). Upon entering a
335 temperature entrainment condition of 12 hr 20 °C: 12 hr 22 °C, the *lnk1/2* mutants were unable to
336 resynchronize their circadian rhythms to that of wild type (**Fig. 5A-B**). This defect was ameliorated
337 when the difference between the minimum and maximum temperature was increased from 2 °C to
338 4 °C; when provided temperature cycles of 12 hr 18 °C: 12 hr 22 °C, most *lnk* mutants were able
339 to realign with the wild-type acrophase (peak reporter expression) by the third day of temperature
340 entrainment (**Fig. 5 C-D**). However, this resynchronization was still slower than when the *lnk*
341 mutants were provided with photocycles—upon the transition from constant light to LD cycles, all
342 mutants were able to immediately re-align their rhythms to wild type, indicating that the *lnk*
343 mutants are specifically impaired in their ability to use temperature as an entrainment cue (**Fig.**
344 **5E-F**).
345 The temperature entrainment programs used in **Figure 5A-D** are non-ramping, meaning
346 the temperature shifts immediately from the cool to warm temperatures. To better simulate
347 environmental conditions, we also employed a ramping, natural temperature entrainment which
348 gradually oscillates between a low temperature of 16 °C and a high of 22 °C. We observed a similar
349 delay in the ability of the *lnk* mutants to assimilate to wild-type acrophase under natural
350 temperature cycles, demonstrating that this defect is not a byproduct of non-ramping temperature
351 changes (**Fig. S8**).
352 As the LNKs form a four-member family, we also examined whether LNK3/4 play a role
353 in temperature entrainment. The *lnk3-1 lnk4-1* double mutant showed little difference from wild-
354 type rhythms under constant light nor temperature entrainment, indicating LNK1/2 are the primary
355 family members important for temperature entrainment (**Fig. S9**). In summary, we have
356 demonstrated a previously unknown role for LNK1/2 in temperature entrainment of the clock.

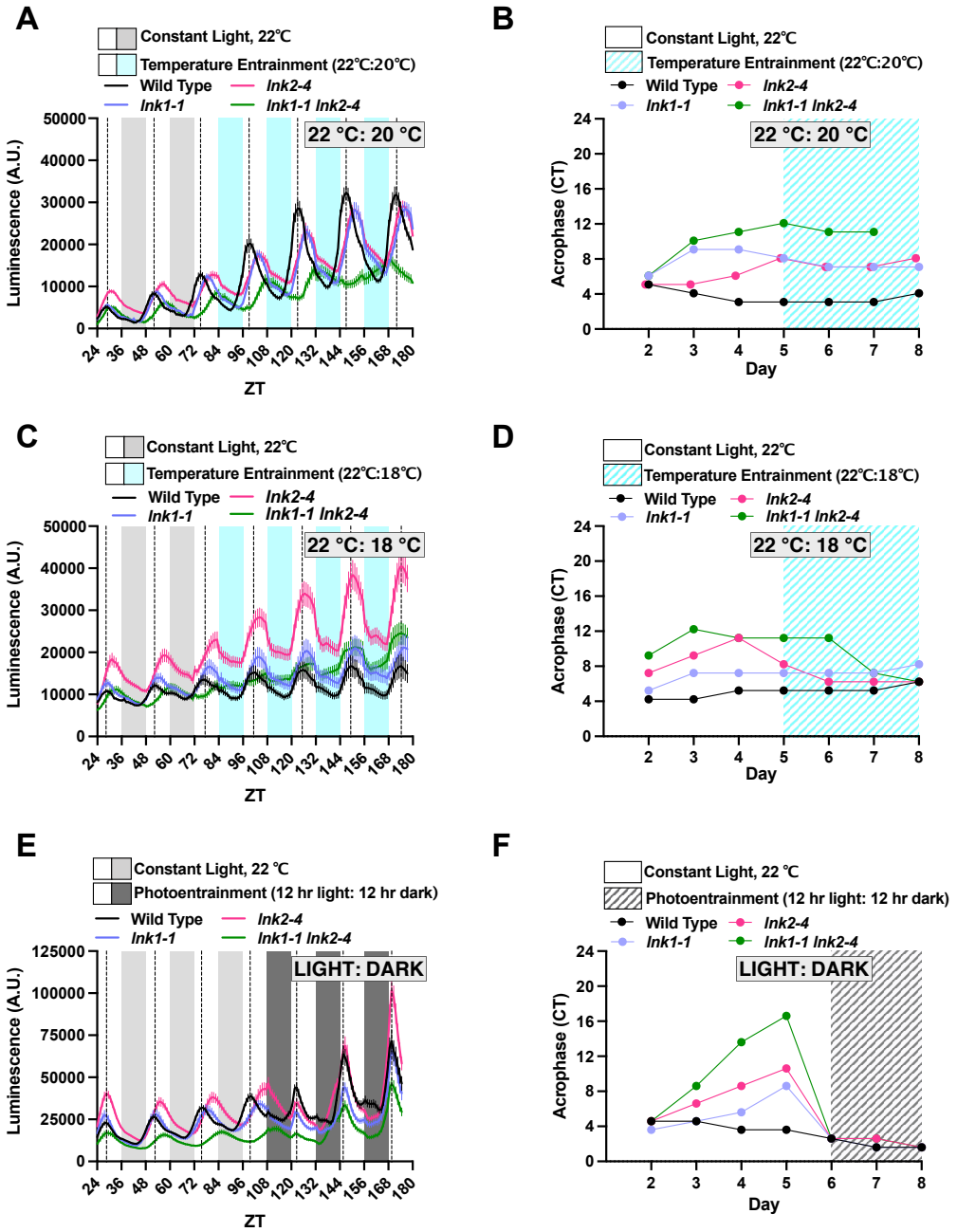

Figure 5 LNK1/2 are important for temperature entrainment of the clock. (A,C,E) Plants were grown for 7 days under 12 hr light: 12 hr dark 22 ℃ conditions for initial entrainment. On day 7, seedlings were transferred to imaging chamber and luminescence was measured for at least 3 days in continuous light and temperature (22 ℃) before the chamber was switched to either a temperature- (A,C) or photo- (E) entrainment program. Temperature entrainment consisted of a day temperature of 22 ℃ and nighttime temperature of 20 ℃ (A) or 18 ℃ (C). Photoentrainment consisted of 12 hr light followed by 12 hr darkness (22 ℃). Lines represent the average luminescence from n=16 seedlings with errors bars = SEM. Vertical dotted lines correspond to the acrophase, or time of peak reporter expression, of the CCA1::LUC reporter in wild type plants. (B,D,F) Acrophase is plotted for each genotype for each day of imaging in constant light and the temperature entrainment condition (B, D) or under photoentrainment (F). Each point represents the acrophase of the averaged luminescence trace shown in (A,C,E). CT = Circadian Time. A.U. = Arbitrary Units. ZT=Zeitgeber Time.

358 **Discussion**

359 Daily and seasonal temperature cycles are important cues for the entrainment of the plant
360 circadian clock (Salomé and Clung, 2005). In parallel to this, the clock is essential for proper
361 response to temperature stimuli (Salomé and Robertson Mcclung, 2005; Thines and Harmon,
362 2010). In this study, we have identified a novel, time-of-day-specific interaction between two
363 established components of the circadian and temperature response pathways: the circadian clock
364 transcriptional activation complex containing RVE8 and LNK1/LNK2 and the cold response
365 proteins COR27/COR28. Previous studies have demonstrated that RVE8 and COR27/COR28 both
366 regulate the transcription of the master cold response regulator *DREB1A* and the core circadian
367 oscillator genes *PRR5* and *TOC1*; however, RVE8 acts as a transcriptional activator of these targets
368 while the CORs act as repressors (Rawat et al., 2011; Li et al., 2016; Wang et al., 2017; Kidokoro
369 et al., 2021). In addition to sharing transcriptional targets, RVE8 and COR27/COR28 also affect
370 similar phenotypes, including period lengthening in the null or knock-down mutants and regulation
371 of photoperiodic flowering time (Rawat et al., 2011; Li et al., 2016). Despite these established
372 overlaps in function between the RVE8-LNK1/LNK2 complex and the CORs, a mechanistic
373 connection between these factors has until now been lacking. In this study, we have demonstrated
374 that COR27/COR28 physically interact with and regulate the protein stability of the RVE8-
375 LNK1/LNK2 complex in the evening and that the CORs antagonize RVE8/LNK1-mediated
376 activation of *TOC1* expression.

377 Our time-of-day-specific APMS experiments demonstrated that RVE8, LNK1, and LNK2
378 interact with different protein partners at ZT5 versus four hours later at ZT9 (**Fig. 2A-D**). LNK1
379 and RVE8 interacted with more protein partners at the later timepoint, ZT9, while LNK2
380 coprecipitated more interactors at ZT5 (**Fig. 2B-D)**. For LNK1 and LNK2, their time of peak
381 protein abundance (**Fig. 1D**) aligned with the time of day when they coprecipitated the most
382 interactors (**Fig. 2B-C**), suggesting that increased abundance of these clock bait proteins led to an
383 increased number of captured interactions. Interestingly, while our 24-hour time course Western
384 blots showed a higher abundance of RVE8-HFC at ZT5, we coprecipitated more interactors at ZT9
385 than at ZT5. This might indicate that even though protein levels of RVE8-HFC are lower at ZT9,
386 perhaps there is an important bridge protein expressed in the evening that links in RVE8-HFC
387 interactors only in the evening. Alternatively, perhaps there are more RVE8-HFC protein
388 interacting partners expressed at ZT9 than at ZT5. By performing APMS at two different time

389 points, we have established that these circadian clock proteins interact with different partners
390 depending on the time of day.

391 For example, COR27, COR28, COP1, and SPA1 were coprecipitated with
392 RVE8/LNK1/LNK2 at ZT9 but not ZT5 (**Tables 1-2**). We have considered the following
393 hypotheses for what is driving this time-of-day-specific interaction: 1) The diurnal expression
394 patterns of these components produces high gene expression overlap at ZT9 but not ZT5, 2) There
395 is a third protein component that is expressed at ZT9 that allows for the interaction between these
396 factors via bridging or by inducing a conformational change in one of the participating proteins,
397 or 3) APMS is not an exclusionary method and could simply have not detected a low abundance
398 peptide that was coprecipitated at ZT5. When we examined the LD mRNA expression patterns for
399 *COR27, COR28, COP1,* and *SPA1*, we found that COR27 and COR28 are most likely ZT9-specific
400 interactors due to their mRNA expression levels having a higher overlap with
401 RVE8/LNK1/LNK2-HFC protein abundance at ZT9 (**Fig. S3**). Indeed, the *CORs* have very low
402 mRNA expression at ZT5 and thus are likely absent from the cell and not interacting with the
403 RVE8-LNK1/2 proteins (**Fig. S3**). COP1 and SPA1, in contrast, do not show higher expression
404 overlap with RVE8-HFC at ZT9 over ZT5 (**Fig. S3**). We instead think it is possible that
405 COP1/SPA1 could be recruited to RVE8 via COR27/COR28 and thus can only be coprecipitated
406 at ZT9 (hypothesis #2). However, future studies are needed to validate this possibility.

407 As COR27/28 are post-translationally regulated by 26S proteasome-mediated degradation
408 (Kahle et al., 2020; Li et al., 2020; Zhu et al., 2020), we predicted that the interaction between
409 RVE8/LNK1/LNK2 and COR27/28 could function to target the circadian transcriptional module
410 for degradation in the evening. We found that RVE8-HFC cyclic protein abundance patterns were
411 disrupted in a *cor27-2 cor28-2* mutant background, with higher RVE8-HFC levels observed
412 specifically during the evening and nighttime hours (**Fig. 4A-C**). This suggests that COR27/28 are
413 important for degradation of RVE8 in the evening. As COP1/SPA1 were also identified as ZT9-
414 specific RVE8 binding proteins, we suggest that the CORs recruit the COP1-SPA1 E3 ubiquitin
415 ligase complex to RVE8-LNK1/2 to target it for degradation by the proteasome, though this has
416 yet to be directly tested. We also coprecipitated *UBIQUITIN-SPECIFIC PROTEASE 12* (*UBP12*)
417 and *UBP13* and the E3 ubiquitin ligases *PLANT U-BOX 12* (*PUB12*) and *PUB13* in
418 RVE8/LNK1/LNK2 APMS experiments and these factors may also play a role in time-of-day-
419 specific complex degradation (**Tables 1-2, Dataset S1**) (Zhou et al., 2021). In tobacco

420 transactivation assays, we observed that presence of COR27/28 reduced the ability of RVE8-
421 LNK1 to activate the expression of a *TOC1* promoter-driven reporter, demonstrating that the CORs
422 have an antagonistic effect on the transcriptional activity of this circadian module (**Fig. 4D**).
423 The CORs do not have identifiable DNA-binding domains and do not bind to DNA *in vitro*
424 (Li et al., 2020); therefore, the CORs must work with a DNA-binding protein to affect transcription
425 of their target genes. Previous work supported this hypothesis by showing that COR27/28 interact
426 with the major photomorphogenic transcription factor ELONGATED HYPOCOTYL 5 (HY5) and
427 regulate some of the same HY5 target loci (Li et al., 2020). Perhaps a similar mechanism is at work
428 here, with the CORs interacting with the RVE-LNK complex to alter its transcriptional activity.
429 The mechanism behind how the CORs change or potentially change the activity of these
430 transcription factors is an open question.
431 Finally, as *COR27/28* expression is induced under cold stress and RVE8 accumulates in
432 the nucleus upon cold treatment, this presents an interesting possibility that the interaction between
433 RVE8 and the CORs could serve to connect cold temperature response and the circadian clock.
434 Notably, COR27/28 and RVE8 oppositely regulate freezing tolerance; the CORs repress
435 expression of *DREB1A* to decrease freezing tolerance while RVE4/8 activate *DREB1A* expression
436 (Li et al., 2016; Kidokoro et al., 2021). Thus, we anticipate that the interaction between the CORs
437 and the RVE8-LNK complex is antagonistic in its nature.
438 In summary, we used affinity purification-mass spectrometry (APMS) to identify novel
439 circadian-associated proteins using the RVE8/LNK1/LNK2 core circadian oscillator proteins as
440 baits. By performing APMS at two time points during the 24-hour cycle, we identified time-of-
441 day-specific interactors, including COR27 and COR28, which only coprecipitated with these three
442 clock baits at the later timepoint, ZT9 **(Fig. 6A, Tables 1 and 2**). The obligate higher order nature
443 of this complex that we established using a yeast 3-hybrid demonstrates a powerful advantage of
444 using an *in vivo* method like APMS over another screening system—screens such as the yeast 2-
445 hybrid library system can only identify binary interactions and thus would never have identified
446 the interaction described here between RVE8, the C-terminus of LNK1, and COR27/28. Taken
447 together, we propose the following model **(Fig. 6B**): In the morning–early afternoon, when the
448 *CORs* are not expressed, the RVE8-LNK1/2 complex is free to perform its canonical duty as an
449 activating force in the circadian oscillator and in cold tolerance. As evening approaches, *COR27*/28
450 expression rises and the RVE8-LNK1/2-COR27/28 complex is formed, which antagonizes RVE8-

LNK1/2 transcriptional activity via regulating RVE8 protein abundance. Future studies examining this complex's role in circadian and cold tolerance phenotypes will be of great interest.

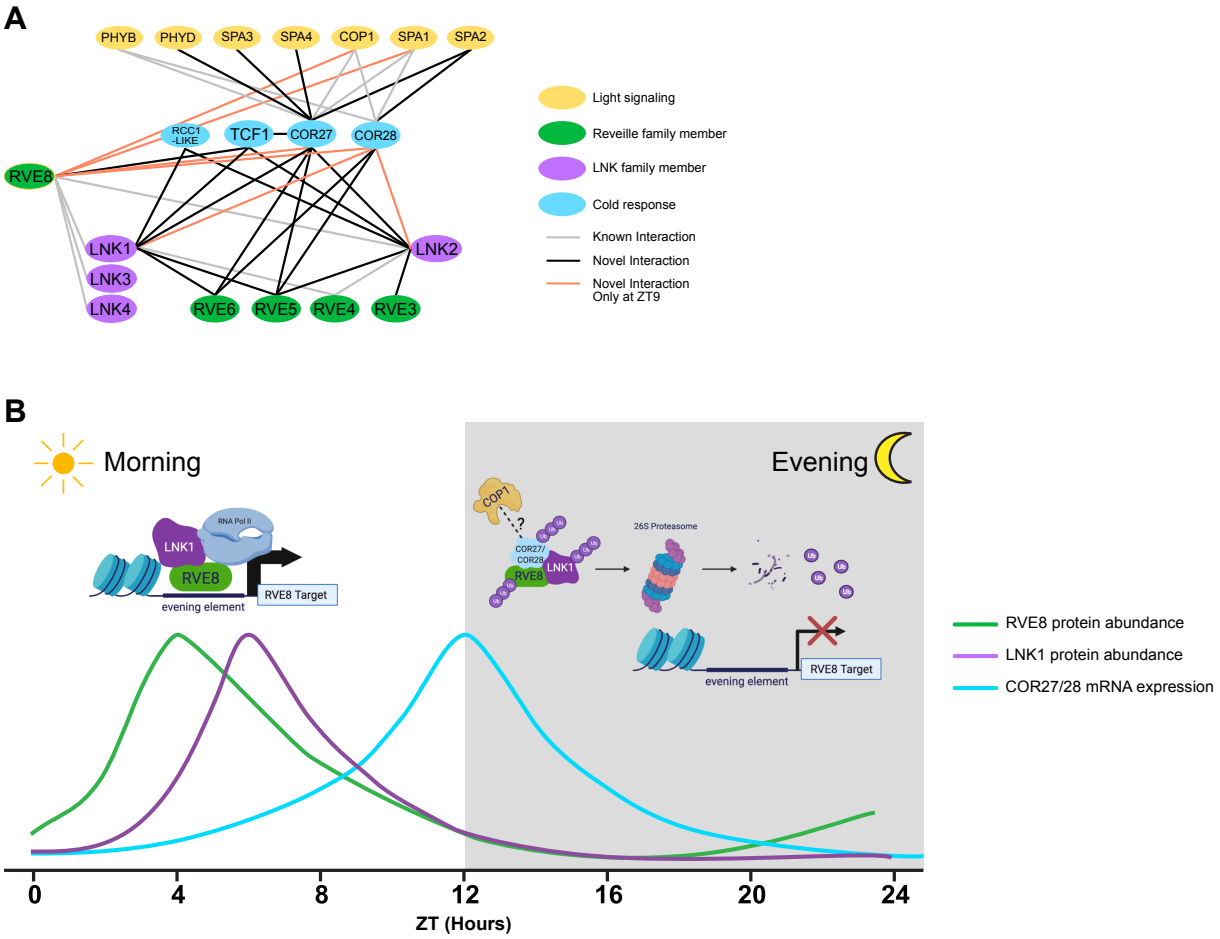

Figure 6 The RVE8-LNK1/2-COR27/28 complex is a novel post-translational regulatory mechanism in the circadian clock. (A) Protein interaction network compiled from APMS experiments using RVE8-HFC, LNK1-HFC, LNK2-HFC, YFP-COR27, and GFP-COR28 as bait proteins at ZT5 and ZT9. Black lines indicate novel interactions identified in this study, grey lines show previously published interactions validated in this study, and orange lines show novel interactions that were identified only at ZT9. (B) Model of hypothesized role of the RVE-LNK-COR interaction during a 24-hour period. In the morning, RVE8-LNK1/2 interact to coactivate the expression of target genes such as evening-phased circadian clock genes and cold-response genes. Towards the evening, COR27/28 are expressed and interact with the RVE8-LNK1/2 complex, potentially recruiting a ubiquitin E3 ligase such as COP1 to target the entire complex for degradation by the 26S proteasome, thus blocking activation of RVE8 targets in the evening. Green and purple lines show approximate protein abundance patterns of RVE8 and LNK1, respectively, while the blue line shows approximate *COR27/28* mRNA expression.

Methods

Plant Materials

T-DNA disrupted lines used in this study: rve8-1 (SALK_053482C), lnk1-1 (SALK_024353), lnk2-1 (GK_484F07), lnk2-4 (GK_484F07), lnk3-1 (SALK_085551C), lnk4-1

458 (GK_846C06), cor27-2 (SALK_042072C), and cor28-2 (SALK_137155C) (Alonso et al., 2003).
459 The lnkQ CCA1::LUC line was generated by transforming the lnkQ mutant background (de Leone
460 et al., 2020) with a binary vector containing CCA1::LUC and Basta resistance (from Harmer Lab).
461 The *lnk3-1 lnk4-1* CCA1::LUC line was generated by crossing *lnk3-1 lnk4-1* to the CCA1::Luc
462 reporter. The 35S::YFP-COR27 and 35S::GFP-COR28 lines were described previously (Li et al.,
463 2016) and generously shared with us by Dr. Hongtao Liu. The rve8-1 CCR2::LUC line was
464 described previously (Rawat et al., 2011) and generously shared with us by Dr. Stacey Harmer.
465 The lnk1-1 CCA1::LUC, lnk2-4 CCA1::LUC, and lnk1-1 lnk2-4 CCA1::LUC lines were a
466 generous gift from Dr. Xiaodong Xu (Xie et al., 2014). All plants used were in the Col-0
467 background.
468 Seeds were gas sterilized and plated on 1/2X Murashige and Skoog basal salt medium with
469 0.8% agar + 1% (w/v) sucrose. After stratification for 2 days, plates were transferred to a Percival
470 incubator (Percival-Scientific, Perry, IA) set to a constant temperature of 22 °C. Light entrainment
471 was 12 hr light/12 hr dark (LD) cycles, with light supplied at 80 μmol/m^2/s. 24-hour tissue
472 collections were performed under white light during the daytime timepoints and under dim green
473 light during the nighttime timepoints.
474
475 **Generation of Epitope-tagged Lines and Plasmid Construction**
476 To generate pB7-RVE8p::RVE8-HFC, RVE8 was cloned from genomic DNA without the stop
477 codon using primers pDAN1127 and pDAN1128 (**Table S2**) and cloned into NotI/AscI-digested
478 pENTR-MCS through In-Fusion HD cloning (Clontech, Mountain View, California). pENTR-
479 RVE8-no stop was then recombined using LR Clonase (Thermo Fisher Scientific, Waltham,
480 Massachusetts) into pB7-HFC (Huang et al., 2016a), which contains the 6X-HIS 3X-FLAG C-
481 terminal tag, to generate pB7-RVE8-HFC. To generate the endogenous promoter driven line, the
482 sequence upstream of the RVE8 transcription start site to the stop codon of the upstream gene was
483 cloned (945 bases) using primers pDAN1129 and pDAN1130 (**Table S2**). The 35S Cauliflower
484 Mosaic Virus (CaMV35S) promoter was excised from pB7-RVE8-HFC via PmeI/SpeI digest and
485 replaced with the RVE8 promoter fragment through In-Fusion HD cloning (Clontech, Mountain
486 View, California) to generate pB7-RVE8P::RVE8-HFC. pB7 RVE8p::RVE8-HFC binary vector
487 was transformed into rve8-1 CCR2::LUC (Rawat et al., 2011) by agrobacterium mediated

488 transformation and positive transformants were identified through basta resistance (Clough and
489 Bent, 1998).
490 To generate pH7WG2-LNK1p::LNK1-HFC and pH7WG2-LNK2p::LNK2-HFC, LNK1 and
491 LNK2 coding sequences were cloned from cDNA without the stop codon using primers
492 pDAN0990/pDAN0991 (LNK1) and pDAN1066/pDAN1067 (LNK2) (**Table S2**) and recombined
493 into pENTR-MCS through dTOPO cloning or In-Fusion HD cloning (Contech, Mountain View,
494 California), respectively. pENTR-LNK1-no stop and pENTR-LNK2-no stop were then
495 recombined using LR Clonase (Thermo Fisher Scientific, Waltham, Massachusetts) into pB7-HFC
496 to generate pB7-LNK1-HFC and pB7-LNK2-HFC. To make the endogenous promoter driven
497 construct, the LNK1 promoter was cloned from the LNK1 transcription start site to the upstream
498 gene's 5' UTR (1709 bp) using primers pDAN1016 and pDAN1017 (**Table S2**). This promoter
499 fragment was swapped with CaMV35S via PmeI/SpeI digest and In-Fusion HD cloning (Clontech,
500 Mountain View, California) to generate pB7-LNK1p::LNK1-HFC. Similarly, the LNK2 promoter
501 was cloned from just before the start of the upstream gene through 142 bases into exon 4 from
502 genomic DNA using primers pDAN1018 and pDAN1019 (**Table S2**) and inserted into pB7-HFC
503 PmeI/BglII digest and In-Fusion HD cloning (Clontech, Mountain View, California) to generate
504 pB7-LNK2p::LNK2-HFC. To make pH7WG2-LNK1p::LNK1-HFC and pH7WG2-
505 LNK2p::LNK2-HFC, pB7-LNK1p::LNK1-HFC, pB7-LNK2p::LNK2-HFC, and pH7WG2
506 (Karimi et al., 2002) were digested with KpnI and AgeI and the resulting fragments were ligated.
507 pH7-LNK1p::LNK1-HFC and pH7-LNK2p::LNK2-HFC binary vector were transformed into
508 lnkQ CCA1::LUC by agrobacterium mediated transformation and positive transformants were
509 identified through hygromycin resistance (Clough and Bent, 1998).
510 To make LNK1 truncations, the N-terminus of LNK1 from the start codon through amino acid
511 296 was cloned using primers pDAN1954/pDAN2010 (**Table S2**), adding a stop codon. The
512 LNK1 C-terminal fragment was cloned using primers pDAN2011/pDAN1955 (**Table S2**) with the
513 first amino acid starting at amino acid number 297. Gene fragments were recombined into pENTR-
514 MCS through In-Fusion HD cloning (Clontech, Mountain View, California) to make pENTR-
515 LNK1-N-term-STOP and pENTR-LNK1-C-term-STOP.
516 To generate pK7-VENUS (VEN)-2x-StrepII-HA-6X-His-C-terminus (SHHc), we first made
517 pK7-SHHc by PCR amplifying the 2X-SII-HA-6X-His C-terminal (SHHc) tag from pB7-SHHc
518 (Huang et al., 2016b) and digesting pK7FWG2 (Karimi et al., 2002) with BstXI and KpnI. The

519 PCR fragment containing the SHHc tag was combined with the digested backbone using In-Fusion
520 HD cloning (Clontech, Mountain View, California) to make pK7-SHHc. Venus was cloned from
521 plasmid mVENUS C1 (Koushik et al., 2006) using primers pDAN0869 and pDAN0870 and
522 recombined with pK7SHHc digested with AvrII using In-Fusion HD cloning (Clontech, Mountain
523 View, California) to generate pK7-VEN-SHHc.

524 pENTR-no stop clones of COR27 and COR28 were generated by amplifying the coding
525 sequences of COR27 (AT5G24900.1) and COR28 (AT4G33980.1) using primers
526 pDAN1906/pDAN1908, and pDAN1909/pDAN1911, respectively (**Table S2**). The resulting
527 amplicons were cloned into NotI/AscI-digested pENTR-MCS through In-Fusion HD cloning
528 (Clontech, Mountain View, California) to make pENTR-COR27-no stop and pENTR-COR28-no
529 stop. To generate pK7-RVE8-VEN-SHHc, pK7-LNK1-VEN-SHHc, pK7-COR27-VEN-SHHc,
530 and pK7-COR28-VEN-SHHc, the pENTR-no stop versions of these genes were recombined to the
531 pK7-VEN-SHHc binary vector using LR Clonase (Thermofisher). These C-terminally tagged
532 proteins are driven from the CaMV35S promoter. To generate the dual luciferase reporter pGreenII
533 0800-LUC-TOC1p, 2098 bp of the TOC1 promoter was cloned using primers
534 pDAN2735/pDAN2736 (**Table S2**) and inserted via In-Fusion HD cloning (Clontech, Mountain
535 View, California) into the pGreenII 0800-LUC plasmid (Hellens et al., 2005) digested with
536 BamHI. The resulting vector (pGreenII 0800-LUC-TOC1p) constitutively expresses renilla
537 luciferase from the CaMV35S promoter and contains the gene for firefly luciferase driven by the
538 TOC1 promoter.

539 To generate yeast 2-/3-hybrid vectors, the gene of interest was cloned from its pENTR-STOP
540 template using primers pDAN2349/pDAN2350 (**Table S2**) and recombined into pGADT7
541 digested with EcoRI using In-Fusion HD cloning (Clontech, Mountain View, California). For
542 cloning into pGBKT7, primers pDAN2347/pDAN2348 (**Table S2**) were used to clone off the
543 pENTR-STOP template and recombine into BamHI-digested pGBKT7 using In-Fusion HD
544 cloning (Clontech, Mountain View, California). For cloning into the pBridge vector (Clontech,
545 Mountain View, California), the gene of interest was cloned from its pENTR-STOP template using
546 primers pDAN2441/pDAN2442 (**Table S2**) and recombined into the first MCS of pBridge
547 digested with EcoRI using In-Fusion HD cloning (Clontech, Mountain View, California) or using
548 primers pDAN2443/pDAN2444 (**Table S2**) to recombine into the second MCS of pBridge
549 digested with BglII using In-Fusion HD cloning (Clontech, Mountain View, California).

550

551

552 **Affinity Purification**

553 Affinity purification was performed as detailed in Sorkin and Nusinow (2022). Briefly,
554 affinity-tagged lines were plated on 1/2x MS + 1% Sucrose and grown for 10 days under LD 22
555 °C conditions. On day 10 of growth, tissue was harvested at either ZT5 or ZT9. To extract protein,
556 powdered tissue was resuspended in SII buffer (100 mM sodium phosphate, pH 8.0, 150 mM NaCl,
557 5 mM EDTA, 5 mM EGTA, 0.1% Triton X-100, 1 mM PMSF, 1x protease inhibitor mixture
558 (Roche, Basel, Switzerland), 1x Phosphatase Inhibitors II & III (Sigma- Aldrich), and 5 µM
559 MG132 (Peptides International, Louisville, KY)) and sonicated using a duty cycle of 20 s (2 s on,
560 2 s off, total of 40 s) at 50% power. Extracts were clarified of cellular debris through 2x
561 centrifugation for 10 min at ≥20,000 × g at 4 °C.

562 For HFC-tagged samples, clarified extracts were incubated with FLAG-M2-conjugated
563 Protein G Dynabeads (Thermo Fisher Scientific, Waltham, Massachusetts) for one hour. Captured
564 proteins were eluted off FLAG beads using 500 µg/mL 3x-FLAG peptide (Sigma-Aldrich). Eluted
565 proteins were then incubated with Dynabeads His-Tag Isolation and Pulldown (Thermo Fisher
566 Scientific, Waltham, Massachusetts) for 20 minutes and then washed 5 x 1 minute in His-tag
567 Isolation Buffer (100 mM Na-phosphate, pH 8.0, 150 mM NaCl, 0.025% Triton X-100). Washed
568 bead pellet was washed 4x in 25mM ammonium bicarbonate and flash frozen in liquid N_2.

569 For YFP-COR27 and GFP-COR28, clarified extracts were incubated with GFP-TRAP
570 Magnetic Agarose affinity beads (ChromoTek GmbH, Planegg-Martinsried, Germany) for one
571 hour. Captured proteins were washed 3 x 1 minute in His-tag Isolation Buffer (100 mM Na-
572 phosphate, pH 8.0, 150 mM NaCl, 0.025% Triton X-100) and 4x in 25mM ammonium bicarbonate
573 and then flash frozen in liquid N_2.

574

575 **LC-MS/MS analysis of AP samples**

576 Samples on affinity beads were resuspended in 50 mM ammonium bicarbonate, reduced
577 (10 mM TCEP) and alkylated (25 mM Iodoacetamide) followed by digestion with Tryspin at 37°C
578 overnight. Digest was separated from beads using a magnetic stand and acidified with 1%TFA
579 before cleaned up with C18 tip (Thermo Fisher Scientific, Waltham, Massachusetts). The extracted
580 peptides were dried down and each sample was resuspended in 10 µL 5% ACN/0.1% FA. 5 µL

581 was analyzed by LC-MS with a Dionex RSLCnano HPLC coupled to a Orbitrap Fusion Lumos
582 mass spectrometer (Thermo Fisher Scientific, Waltham, Massachusetts) using a 2h gradient.
583 Peptides were resolved using 75 µm x 50 cm PepMap C18 column (Thermo Fisher Scientific,
584 Waltham, Massachusetts).
585 Peptides were eluted at 300 nL/min from a 75 µm x 50 cm PepMap C18 column (Thermo
586 Scientific) using the following gradient: Time = 0–4 min, 2% B isocratic; 4–8 min, 2–10% B; 8–
587 83 min, 10–25% B; 83–97 min, 25–50% B; 97–105 min, 50–98%. Mobile phase consisted of A,
588 0.1% formic acid; mobile phase B, 0.1% formic acid in acetonitrile. The instrument was operated
589 in the data-dependent acquisition mode in which each MS1 scan was followed by Higher-energy
590 collisional dissociation (HCD) of as many precursor ions in 2 second cycle (Top Speed method).
591 The mass range for the MS1 done using the FTMS was 365 to 1800 m/z with resolving power set
592 to 60,000 @ 400 m/z and the automatic gain control (AGC) target set to 1,000,000 ions with a
593 maximum fill time of 100 ms. The selected precursors were fragmented in the ion trap using an
594 isolation window of 1.5 m/z, an AGC target value of 10,000 ions, a maximum fill time of 100 ms,
595 a normalized collision energy of 35 and activation time of 30 ms. Dynamic exclusion was
596 performed with a repeat count of 1, exclusion duration of 30 s, and a minimum MS ion count for
597 triggering MS/MS set to 5000 counts.
598
599 **AP-MS Data Analysis**
600 MS data were converted into mgf. Database searches were done using Mascot (Matrix
601 Science, London, UK; v.2.5.0) using the TAIR10 database (20101214, 35,386 entries) and the
602 cRAP database (http://www.thegpm.org/cRAP/) and assuming the digestion enzyme trypsin and
603 2 missed cleavages. Mascot was searched with a fragment ion mass tolerance of 0.60 Da and a
604 parent ion tolerance of 10 ppm. Oxidation of methionine and carbamidomethyl of cysteine were
605 specified in Mascot as variable modifications. Scaffold (Proteome Software Inc., Portland, OR;
606 v.4.8) was used to validate MS/MS based peptide and protein identifications. Peptide
607 identifications were accepted if they could be established at greater than 95.0% probability by the
608 Peptide Prophet algorithm (Keller et al., 2002) with Scaffold delta-mass correction. The Scaffold
609 Local FDR was used and only peptides probabilities with FDR $<$1% were used for further analysis.
610 Protein identifications were accepted if they could be established at greater than 99.9% probability
611 as assigned by the Protein Prophet algorithm (Nesvizhskii et al., 2003). Proteins that contained

612 similar peptides and could not be differentiated based on MS/MS analysis alone were grouped to
613 satisfy the principles of parsimony. Proteins sharing significant peptide evidence were grouped
614 into clusters. Only the proteins identified with ≥ 2 unique peptides were further used in the analysis,
615 except when proteins with only one peptide were identified in more than one replicate.
616

617 **Yeast 2-Hybrid (Y2H) and Yeast 3-Hybrid Assays**

618 We used the GAL4-based Matchmaker Gold Yeast 2-Hybrid System (Clontech, Mountain
619 View, California) for all Y2H and Y3H assays. All transformations were performed as detailed in
620 the Yeast Protocols Handbook (Clontech, Mountain View, California). For Y2H, bait proteins
621 were cloned into the pGBKT7 vector which encodes the GAL4 DNA binding domain and then
622 transformed into the Y2H Gold strain (Clontech, Mountain View, California) and plated on SD/-
623 Trp to select for positive transformants. Prey proteins were cloned into the pGADT7 vector which
624 encodes the GAL4 activation domain, transformed into the Y187 strain (Clontech, Mountain View,
625 California), and plated on SD/-Leu to select for positive transformants. All matings were
626 performed as detailed in the Yeast Protocols Handbook (Clontech, Mountain View, California)
627 using the 96-well plate format. Mated diploids were selected for on SD/-Leu/-Trp media. Single
628 colonies of mated bait + prey strains were resuspended in YPDA and plated on SD/-Leu-Trp or
629 SD/-Leu-Trp-His plates.

630 For Y3H, bait and linker proteins were cloned into the appropriate position of the pBridge
631 vector (Clontech, Mountain View, California), which encodes a GAL4 DNA binding domain and
632 a linker protein, transformed into the Y2H Gold strain, and plated on SD/-Trp to select for positive
633 transformants. pBridge strains were mated with pGADT7 prey strains and plated on SD/-Trp/-Leu
634 to select for diploids. Single colonies of mated strains were resuspended in YPDA plated on SD/-
635 Leu-Trp or SD/-Leu-Trp-His plates.
636

637 **Luciferase Reporter Assays**

638 Individual 6-day-old seedlings expressing a CCA1::LUC reporter grown under LD cycles
639 at 22°C were arrayed on 1/2x MS + 1% Sucrose plates and sprayed with 5mM luciferin (GoldBio,
640 Olivette, MO) prepared in 0.01% (v/v) Triton X-100 (Millipore Sigma-Aldrich, St. Louis, MO).
641 Plants were transferred to an imaging chamber set to the appropriate free-run or entrainment
642 program and images were taken every 60 minutes with an exposure of 10 minutes after a 3-minute

643 delay after lights-off to diminish signal from delayed fluorescence using a Pixis 1024 CCD camera
644 (Princeton Instruments, Trenton, NJ). Images were processed to measure luminescence from each
645 plant using the Metamorph imaging software (Molecular Devices, Sunnyvale, CA). Circadian
646 period was calculated using fast Fourier transformed nonlinear least squares (FFT-NLLS) (Plautz
647 et al., 1997) using the Biological Rhythms Analysis Software System 3.0 (BRASS) available at
648 http://www.amillar.org.
649

650 ***N. benthamiana* Transient Transformation**

651 Transient transformation of 3-4 week-old *N. benthamiana* plants was performed as in
652 (Lasierra and Prat, 2018). Briefly, overnight saturated cultures of *Agrobacterium tumefaciens*
653 strain GV3101 carrying pGreenII 0800-LUC-TOC1p, pK7-RVE8-VEN-SHHc, pK7-LNK1-VEN-
654 SHHc, pK7-COR27-VEN-SHHc, pK7-COR28-VEN-SHHc, or 35S::P19-HA (Chapman et al.,
655 2004) were pelleted and resuspended in 5 mL of resuspension buffer (10mM $MgSO_4$, 10mM MES
656 (pH 5.8), 150 µM Acetosyringone) for 2-3 hours. Cultures were diluted to OD_{600}= 0.4 in
657 resuspension buffer and inoculation mixtures were prepared by mixing the selected constructs
658 together with the volume of 35S::P19-HA being varied to ensure that an equal amount of
659 agrobacteria was added to each mixture relative to the reporter, regardless of the total number of
660 effectors being introduced. Mixtures were inoculated into one quadrant of a mature leaf per one
661 mixture. Four different mixtures could be inoculated into a single leaf. Three leaves per plant were
662 inoculated and four plants were used for a total of 12 biological replicates per mixture.
663

664 **Dual-Luciferase Assay**

665 The dual luciferase assay was performed using the Dual-Glo Luciferase Assay System
666 (Promega, Madison, Wisconsin). Briefly, 3-4 week-old tobacco plants were inoculated with
667 *Agrobacterium tumefaciens* expressing pGreenII 0800-LUC-TOC1p and a combination of other
668 proteins: pK7-RVE8-VEN-2x-StrepII-HA-6X-His-C-terminus (SHHc), pK7-LNK1-VEN-SHHc,
669 pK7-COR27-VEN-SHHc, or pK7-COR28-VEN-SHHc. This reporter firefly luciferase driven by
670 the 3 leaf disks were collected per infiltration site from 3-day-post-infiltrated tobacco plants and
671 frozen in liquid N_2. Tissue was homogenized and resuspended in 200 µL of Cell Culture Lysis
672 Reagent (100 mM potassium phosphate, pH 7.8, 1 mM EDTA, 7mM 2-mercaptoethanol, 1%
673 Triton X-100, 10% glycerol). Lysates were centrifuged at max speed for 5 minutes and 5 µL of

674 undiluted extract was used for the Dual Luciferase Assay input. 40 µL of Luciferase Assay Buffer
675 was added to undiluted extract in a black 96-well plate and incubated for at least 10 minutes.
676 Luminescence was measured over a 10-minute exposure using a Pixis 1024 CCD camera
677 (Princeton Instruments, Trenton, NJ). 40 µL of Stop & Glo Reagent was added to wells to quench
678 the firefly luciferase signal and provide the substrate for renilla luciferase. After at least 10 minutes
679 incubation, luminescence was measured over a 10-minute exposure using the CCD camera. Firefly
680 luciferase signal was divided by renilla signal to calculate normalized luminescence.
681
682 **Densitometry Analysis**
683 Densitometry analysis was performed in FIJI (https://imagej.net/software/fiji/) on high
684 resolution (600 dpi), greyscale images of Western blots captured with the same exposure time.
685 Mean grey value was measured from ROIs of equal area for each protein band and for background
686 regions as well as for loading controls (Ponceau S stain) and loading control background regions.
687 Inverted pixel density of background regions was subtracted from the inverted pixel density of
688 protein bands and loading controls to generate the net pixel density value. To calculate normalized
689 abundance, the ratio of the net protein band value over the net loading control value was taken.
690
691 **Quantitative RT-PCR**
692 Seedlings were gas sterilized and grown on 1/2x MS + 1% Sucrose plates with Whatman
693 filter paper under 12 hr light: 12 hr dark, 22 °C conditions. On day 7 of growth at ZT10, plates
694 were transferred to a different chamber set to either 22 °C or 4 °C for two hours. Tissue was
695 collected at ZT12. Total RNA was extracted from powdered tissue using the RNeasy Plant Mini
696 kit (Qiagen, Hilden, Germany). 1 µg of total RNA was used as the template to synthesize cDNA
697 using the iScript RT-PCR kit (Bio-Rad, Carlsbad, CA). qPCR was performed with the SYBR
698 Green I nucleic acid gel stain (Sigma-Aldrich) using a QuantStudio 5 Real-Time PCR System
699 (ThermoFisher). PCR was set up as follows: 3 min at 95˚C, followed by 40 cycles of 10 s at 95˚C,
700 10 s at 55˚C and 20 s at 72˚C. A melting curve analysis was conducted right after all PCR cycles
701 are done. APA1 (At1g11910), expression of which remain stable during the diurnal cycle, was
702 used as the normalization control. Primers for qPCR are listed in **Table S2**.
703
704 **Acknowledgements**

We acknowledge support by the National Science Foundation under Grant No. DBI-1827534 for acquisition of the Orbitrap Fusion Lumos LC-MS/MS and from the NIH award 5R01GM141374 to DAN. MLS was supported by NSF GRF award DGE-1745038 and by the William H. Danforth Plant Science Fellowship from the Donald Danforth Plant Science Center. This study was also supported by the German Research Foundation (DFG) under Germany's Excellence Strategy (CIBSS - EXC 2189 – Project ID 390939984) and DFG grant HI 1369/6-1 to AH and by Agencia Nacional de Promoción Científica y Tecnológica (ANPCyT) to MJY.

Author Contributions

MLS, NK, AH, MJY, AR, BSE and DAN designed the research project. The research was performed by MLS, ST, and RB. AR contributed new analysis to the paper. MLS, ST, and DAN wrote the paper.

Figure Legends

Figure 1 Characterization of affinity-tagged lines used for APMS (A-C) Circadian luciferase reporter period analysis of selected T3 homozygous lines expressing (A) LNK1-HFC, (B) LNK2-HFC, or (C) RVE8-HFC in their respective mutant backgrounds (*rve8-1* or *lnkQ*). Each point represents the circadian period of an individual plant and the + symbol shows the average period for that genotype. Letters correspond to significantly different periods as determined by ANOVA with a Tukey's post-hoc test. LNK1 and LNK2 luciferase assays were performed together and include the same wildtype and *lnkQ* data. Environmental conditions during imaging are included at the top of the plot (LL = constant light). (D-F) Time course Western blots showing cyclic protein abundance patterns of 10-day-old affinity tagged lines under 12 hr light: 12 hr dark 22 °C conditions. Affinity tagged lines are detected with anti-FLAG antibody. RPT5 or Ponceau S staining was used to show loading. Col-0 CCA1::LUC (Col-0) or *rve8-1* CCR2::LUC (*rve8-1*) were used as negative controls. White and black bars indicate lights-on and lights-off, respectively (D) 24-hour protein expression patterns of affinity tagged lines normalized to Ponceau S or RPT5 quantified by densitometry of Western blots shown in D-F. Vertical dotted lines indicate time of tissue collection for APMS. White and grey shading indicates lights-on and lights-off, respectively. Western blots and luciferase reporter assays were repeated at least 2 times. ZT= Zeitgeber Time.

Figure 2 Analysis of proteins coprecipitated with RVE8/LNK1/LNK2-HFC by time-of-day affinity purification-mass spectrometry (A) Venn diagram showing number of proteins coprecipitated with RVE8/LNK1/LNK2 at ZT5, ZT9, or at both timepoints. Corresponding bar charts show enriched GO biological process terms with $-\text{Log10}_{(\text{p-value})}$. (B-D) Venn diagrams of coprecipitated proteins at ZT5 and ZT9 separated by bait protein (B, LNK1-HFC, C, LNK2-HFC, or D, RVE8-HFC). (E-H) mRNA expression profiles in constant light of four cold-response proteins identified as RVE8/LNK1/LNK2 interactors. RNA-seq data for E-H taken from Romanowski et al. (2020) *The Plant Journal*. ZT= Zeitgeber Time

744
745 **Figure 3 COR27/28 interact with RVE8/LNK1 in a yeast 3-hybrid system** Yeast strains Y2H
746 Gold or Y187 expressing pBridge (GAL4-DBD and a Bridge protein) or pGADT7 (GAL4-AD),
747 respectively, were mated and plated onto selective media. Successful matings can grow on -
748 Leucine/-Tryptophan media (-L-W) while positive interactors can grow on -Leucine/-Tryptophan/-
749 Histidine + 2mM 3-amino-1,2,4-triazole (3AT) (-L-W-H + 2mM 3AT). A graphical depiction of
750 different combinations is shown to the right. AD-T (large T-antigen protein) is a negative control
751 for prey interactions. Experiment was repeated at least twice.
752
753 **Figure 4 COR27/28 alter RVE8-HFC protein abundance patterns and inhibit RVE8/LNK1-**
754 **mediated activation of *TOC1*** (A-B) 24-hour protein expression patterns of RVE8-HFC in wild
755 type (A) or *cor27-2 cor28-2* (B) backgrounds analyzed by Western blot. Tissue was collected
756 every 3 hours from 12-day-old plants grown under 12 hr light: 12 hr dark 22 °C conditions. Anti-
757 FLAG antibody was used to detect RVE8-HFC and Ponceau S staining was used to show loading.
758 White and black bars indicate lights-on and lights-off, respectively. Col-0 CCR2::LUC was used
759 as the negative control. (C) Densitometry quantification of (A) and (B) RVE8-HFC 24-hour
760 abundance normalized to Ponceau S in wild type and *cor27-2 cor28-2* backgrounds. Points
761 represent the average normalized RVE8-HFC abundance from 3 (WT) or 4 (*cor27-2 cor28-2*)
762 independent bioreps. Asterisks indicate significant differences between genotypes based on
763 Welch's t-test (* $p< 0.05$). Error bars = SD. (D) Dual luciferase assay in 3–4-week-old *Nicotiana*
764 *benthamiana*. Schematic of expression constructs infiltrated are shown at the top (SHH = 2X-
765 StrepII-HA-His_6 tag). Luminescence from a dual firefly/renilla luciferase reporter was measured
766 after coinfection with 35S::RVE8-VENUS-SHH, 35S::LNK1-VENUS-SHH, 35S::COR27-
767 VENUS-SHH, or 35S::COR28-VENUS-SHH. Luminescence was normalized to constitutively
768 expressed renilla luciferase luminescence to control for infection efficiency. Points represent the
769 normalized luminescence from 3-4 independent experiments with N=12. Mean normalized
770 luminescence is indicated by the crosshair symbol and error bars = SD. Asterisks indicate
771 significant differences by unpaired t-test with Welch correction (ns= not significant, * $p< 0.05$, **
772 $p< 0.01$). ZT= Zeitgeber Time. Empty = reporter alone.
773
774 **Figure 5 LNK1/2 are important for temperature entrainment of the clock.** (A,C,E) Plants
775 were grown for 7 days under 12 hr light: 12 hr dark 22 °C conditions for initial entrainment. On
776 day 7, seedlings were transferred to imaging chamber and luminescence was measured for at least
777 3 days in continuous light and temperature (22 °C) before the chamber was switched to either a
778 temperature- (A,C) or photo- (E) entrainment program. Temperature entrainment consisted of a
779 day temperature of 22 °C and nighttime temperature of 20 °C (A) or 18 °C (C). Photoentrainment
780 consisted of 12 hr light followed by 12 hr darkness (22 °C). Lines represent the average
781 luminescence from n=16 seedlings with errors bars = SEM. Vertical dotted lines correspond to the
782 acrophase, or time of peak reporter expression, of the CCA1::LUC reporter in wild type plants.
783 (B,D,F) Acrophase is plotted for each genotype for each day of imaging in constant light and the
784 temperature entrainment condition (B, D) or under photoentrainment (F). Each point represents
785 the acrophase of the averaged luminescence trace shown in (A,C,E). CT = Circadian Time. A.U.
786 = Arbitrary Units. ZT=Zeitgeber Time.
787
788 **Figure 6 The RVE8-LNK1/2-COR27/28 complex is a novel post-translational regulatory**
789 **mechanism in the circadian clock.** (A) Protein interaction network compiled from APMS

experiments using RVE8-HFC, LNK1-HFC, LNK2-HFC, YFP-COR27, and GFP-COR28 as bait proteins at ZT5 and ZT9. Black lines indicate novel interactions identified in this study, grey lines show previously published interactions validated in this study, and orange lines show novel interactions that were identified only at ZT9. (B) Model of hypothesized role of the RVE-LNK-COR interaction during a 24-hour period. In the morning, RVE8-LNK1/2 interact to coactivate the expression of target genes such as evening-phased circadian clock genes and cold-response genes. Towards the evening, COR27/28 are expressed and interact with the RVE8-LNK1/2 complex, potentially recruiting a ubiquitin E3 ligase such as COP1 to target the entire complex for degradation by the 26S proteasome, thus blocking activation of RVE8 targets in the evening. Green and purple lines show approximate protein abundance patterns of RVE8 and LNK1, respectively, while the blue line shows approximate *COR27/28* mRNA expression.

Supplemental Figure 1 mRNA expression patterns of *RVE8*, *LNK1*, or *LNK2* under photocycles (12 hr light: 12 hr dark). White and dark grey shading indicates lights-on and lights-off, respectively. Microarray data from diurnal.mocklerlab.com.

Supplemental Figure 2 Protein alignment of TCF1 (AT3G55580) and RCC1L (AT3G53830). Protein sequences were aligned using the needle algorithm using the EBLOSUM62 matrix, a gap penalty of 10.0, and an extend penalty of 0.5. Sequences share 49.7% identity.

Supplemental Figure 3 Comparison of HFC-tagged protein abundance with *COR27/28*, *COP1*, and *SPA1* mRNA expression profiles. 24-hour (12 hr light: 12 hr dark, 22 ℃ (LDHH)) protein abundance (dark blue) is quantified from Western blots shown in Figure 1D-F. LDHH mRNA data from diurnal.mocklerlab.com (light blue) is overlayed. Vertical dotted lines show the time of day when tissue was collected for APMS. White and grey shading indicated lights-on and lights-off, respectively.

Supplemental Figure 4 COR27/28 do not interact with RVE8 or LNK1 in a binary Y2H system Yeast strains Y2H Gold or Y187 expressing pGBKT7 (Gal4-DBD) or pGADT7 (Gal4-AD), respectively, were mated and plated onto selective media. Successful matings were able to grow on -Leucine/-Tryptophan media (-L-W) while positive interactors can grow on -Leucine/-Tryptophan/-Histidine + 2mM 3-amino-1,2,4-triazole (3AT) (-L-W-H +3AT). Only the positive controls DBD-53 (p53) + AD-T (large T-antigen protein) and DBD-RVE8 + AD-LNK1 C-term show an interaction.

Supplemental Figure 5 Full-length LNK1 auto-activates in yeast when paired with a DBD-containing protein Yeast strains Y2H Gold or Y187 expressing pBridge (Gal4-DBD and a Bridge protein) or pGADT7 (Gal4-AD), respectively, were mated and plated onto selective media. Successful matings were able to grow on -Leucine/-Tryptophan media (-L-W). Full length LNK1 (bridge protein, no AD domain) paired with the transcription factor RVE8 (*) can aberrantly activate the expression of the histidine biosynthesis reporter, allowing it to grow on -Leucine/-Tryptophan/-Histidine (-L-W-H) when paired with the negative control large T-antigen protein (T). LNK1 N- and C-terminal truncations do not autoactivate.

Supplemental Figure 6 RVE8-HFC protein abundance patterns are regulated by the 26S proteasome (A) Representative Western blot showing protein expression patterns of RVE8-HFC

836 plants treated with DMSO or 100 µM bortezomib. At ZT5, 12-day-old seedlings growing under
837 12 hr light: 12 hr dark, 22 °C conditions were immersed in 1/2X MS media containing either 100
838 µM bortezomib or DMSO. Tissue was collected every 3 hours starting at ZT6. RVE8-HFC was
839 detected with anti-FLAG and Ponceau S staining was used to show loading. (B) Densitometry
840 quantification of RVE8-HFC abundance in (A) normalized to Ponceau S. Points represent the
841 average normalized RVE8-HFC abundance from 3 independent bioreps. Asterisks indicate
842 significant differences between genotypes based on Welch's t-test (* $p<0.05$). Error bars = SD.
843 White and grey shading indicate lights-on and lights-off, respectively. ZT= Zeitgeber Time.
844
845 **Supplemental Figure 7 The RVEs and LNKs are important for cold induction of *COR27/28*.**
846 Seedlings were grown on 1/2X MS + 1% sucrose for seven days under 12 hr light; 12 hr dark 22
847 °C conditions and then transferred at ZT10 to either 22 °C or 4 °C for two hours and tissue was
848 collected at ZT12. (A-B) show the induction of *COR27/28* expression at 4 °C compared to 22 °C.
849 Figures (C-D) show *COR27/28* expression levels at 22 °C. Expression was normalized to the
850 endogenous control gene APA1. Bars show average expression with error bars = SD from 3
851 independent bioreps (points) for each genotype. Asterisks indicate significant differences as
852 determined by Welch's t-test (** $p<0.01$, *** $P<0.001$).
853
854 **Supplemental Figure 8 LNK1/2 mutants are also impaired in temperature entrainment**
855 **under ramping temperature cycles** (A) Luminescence from 7-day-old plants entrained under 12
856 hr light: 12 hr dark, 22 °C conditions expressing a CCA1p::LUC reporter was imaged for at least
857 3 days in continuous light and temperature (22 °C) before the chamber was switched to a ramping
858 temperature entrainment program that gradually oscillated between a low temperature of 16 °C at
859 ZT16 and a high of 22 °C at ZT4. Lines represent the average luminescence from n=16 seedlings
860 with errors bars = SEM. Vertical dotted lines correspond to the peak expression time (acrophase)
861 of the CCA1p::LUC reporter in wild type plants. (B) Acrophase, or time of peak reporter
862 expression, is plotted for each genotype for each day of imaging in constant light and the
863 temperature entrainment condition. Each point represents the acrophase of the averaged
864 luminescence trace shown in (A). CT = Circadian Time. A.U. = Arbitrary Units. ZT= Zeitgeber
865 Time.
866
867 **Supplemental Figure 9 *lnk3/4* mutants are not impaired in temperature entrainment** (A)
868 Luminescence from 7-day-old plants expressing a CCA1p::LUC reporter were grown for at least
869 3 days in continuous light and temperature (22 °C) before the chamber was switched to a ramping
870 temperature entrainment program that gradually oscillates between a low temperature of 16 °C at
871 ZT16 and a high of 22 °C at ZT4. Lines represent the average luminescence from n=16 seedlings
872 with errors bars = SEM. Vertical dotted lines correspond to the peak expression time of the
873 CCA1p::LUC reporter in wild type plants. (B) Acrophase, or time of peak reporter expression, is
874 plotted for each genotype for each day of imaging in constant light and the temperature entrainment
875 condition. Each point represents the acrophase of the averaged luminescence trace shown on the
876 right. CT = Circadian Time. A.U. = Arbitrary Units. ZT=Zeitgeber Time.
877
878 **Table 1 Proteins coprecipitated with RVE8/LNK1/LNK2-HFC at ZT5.** Total spectra for a
879 given coprecipitated protein is shown for each independent ZT5 sample. The curated table
880 excludes coprecipitated proteins that were identified in the GFP-HFC or Col-0 negative control
881 APMS experiments, see Dataset S1 for all identifications.

882
883 **Table 2 Identified proteins coprecipitated with RVE8/LNK1/LNK2-HFC at ZT9.** Total
884 spectra for a given coprecipitated protein is shown for each independent ZT9 sample. The curated
885 table excludes coprecipitated proteins that were identified in the GFP-HFC or Col-0 negative
886 control APMS experiments, see Dataset S1 for all identifications.
887
888 **Table 3 Identified proteins coprecipitated with YFP-COR27/GFP-COR28 at ZT9.** Total
889 spectra for a given coprecipitated protein is shown for each independent ZT9 sample. The curated
890 table excludes coprecipitated proteins that were identified in the GFP-HFC or Col-0 negative
891 control APMS experiments, see Dataset S1 for all identifications.
892
893 **Supplemental Table 1 *AT3G53830* (*RCC1L*) is downregulated at 4 °C**. Data taken from
894 Kidokoro et al. (2021) PNAS. Wild-type (Col-0) plants were transferred to 4 °C at LL2 (T=0; 2
895 hours after dawn) and tissue for RNA sequencing was collected at 3 hours and 12 hours after
896 transfer to cold conditions. *RCC1L* is significantly downregulated after 12 hours under 4 °C
897 treatment.
898
899 **Supplemental Table 2 Oligonucleotides used in this study.**
900

901 **References**

902 **Alonso JM, Stepanova AN, Leisse TJ, Kim CJ, Chen H, Shinn P, Stevenson DK,**
903 **Zimmerman J, Barajas P, Cheuk R, et al** (2003) Genome-wide insertional mutagenesis
904 of Arabidopsis thaliana. Science (80-) **301**: 653–657
905 **Avello PA, Davis SJ, Ronald J, Pitchford JW** (2019) Heat the Clock: Entrainment and
906 Compensation in *Arabidopsis* Circadian Rhythms. J Circadian Rhythms **17**: 5
907 **Blair EJ, Bonnot T, Hummel M, Hay E, Marzolino JM, Quijada IA, Nagel DH** (2019)
908 Contribution of time of day and the circadian clock to the heat stress responsive
909 transcriptome in Arabidopsis. Sci Rep **9**: 4814
910 **Chapman EJ, Prokhnevsky AI, Gopinath K, Dolja V V., Carrington JC** (2004) Viral RNA
911 silencing suppressors inhibit the microRNA pathway at an intermediate step. Genes Dev **18**:
912 1179
913 **Clough SJ, Bent AF** (1998) Floral dip: A simplified method for Agrobacterium-mediated
914 transformation of Arabidopsis thaliana. Plant J **16**: 735–743
915 **Devlin PF, Kay SA** (2001) CIRCADIAN PHOTOPERCEPTION. Annu Rev Physiol **63**: 677–
916 694
917 **Gray JA, Shalit-Kaneh A, Chu DN, Yingshan Hsu P, Harmer SL** (2017) The REVEILLE
918 Clock Genes Inhibit Growth of Juvenile and Adult Plants by Control of Cell Size. Plant

919 Physiol **173**: 2308–2322
920 **Hellens RP, Allan AC, Friel EN, Bolitho K, Grafton K, Templeton MD, Karunairetnam S,**
921 **Gleave AP, Laing WA** (2005) Transient expression vectors for functional genomics,
922 quantification of promoter activity and RNA silencing in plants. doi: 10.1186/1746-4811-1-
923 13
924 **Hooper CM, Tanz SK, Castleden IR, Vacher MA, Small ID, Millar AH** (2014) Data and text
925 mining SUBAcon: a consensus algorithm for unifying the subcellular localization data of
926 the Arabidopsis proteome. **30**: 3356–3364
927 **Hsu PY, Devisetty UK, Harmer SL** (2013a) Accurate timekeeping is controlled by a cycling
928 activator in Arabidopsis. Elife **2**: e00473
929 **Hsu PY, Devisetty UK, Harmer SL** (2013b) Accurate timekeeping is controlled by a cycling
930 activator in Arabidopsis. Elife. doi: 10.7554/eLife.00473
931 **Huang H, Alvarez S, Bindbeutel R, Shen Z, Naldrett MJ, Evans BS, Briggs SP, Hicks LM,**
932 **Kay SA, Nusinow DA, et al** (2016a) Identification of Evening Complex Associated
933 Proteins in Arabidopsis by Affinity Purification and Mass Spectrometry. Mol Cell
934 Proteomics **15**: 201–217
935 **Huang H, Yoo CY, Bindbeutel R, Goldsworthy J, Tielking A, Alvarez S, Naldrett MJ,**
936 **Evans BS, Chen M, Nusinow DA** (2016b) PCH1 integrates circadian and light-signaling
937 pathways to control photoperiod-responsive growth in Arabidopsis. Elife **5**: 1–27
938 **Ji H, Wang Y, Cloix C, Li K, Jenkins GI, Wang S, Shang Z, Shi Y, Yang S, Li X** (2015) The
939 Arabidopsis RCC1 Family Protein TCF1 Regulates Freezing Tolerance and Cold
940 Acclimation through Modulating Lignin Biosynthesis. PLOS Genet **11**: e1005471
941 **Kahle N, Sheerin DJ, Fischbach P, Koch LA, Schwenk P, Lambert D, Rodriguez R, Kerner**
942 **K, Hoecker U, Zurbriggen MD, et al** (2020) COLD REGULATED 27 and 28 are targets
943 of CONSTITUTIVELY PHOTOMORPHOGENIC 1 and negatively affect phytochrome B
944 signalling. Plant J **104**: 1038–1053
945 **Karimi M, Inzé D, Depicker A** (2002) GATEWAY^{TM} vectors for Agrobacterium-mediated
946 plant transformation. Trends Plant Sci **7**: 193–195
947 **Keller A, Nesvizhskii AI, Kolker E, Aebersold R** (2002) Empirical statistical model to
948 estimate the accuracy of peptide identifications made by MS/MS and database search. Anal
949 Chem **74**: 5383–5392

950 **Kidokoro S, Hayashi K, Haraguchi H, Ishikawa T, Soma F, Konoura I, Toda S, Mizoi J,**
951 **Suzuki T, Shinozaki K, et al** (2021) Posttranslational regulation of multiple clock-related
952 transcription factors triggers cold-inducible gene expression in Arabidopsis. Proc Natl Acad
953 Sci. doi: 10.1073/PNAS.2021048118
954 **Koushik S V, Chen H, Thaler C, Puhl HL 3rd, Vogel SS** (2006) Cerulean, Venus, and
955 VenusY67C FRET reference standards. Biophys J **91**: L99–L101
956 **Lasierra P, Prat S** (2018) Transient Transactivation Studies in Nicotiana benthamiana Leaves.
957 *In* L Oñate-Sánchez, ed, Two-Hybrid Syst. Methods Protoc. Springer New York, New
958 York, NY, pp 311–322
959 **de Leone MJ, Hernando CE, Romanowski A, García-Hourquet M, Careno D, Casal J,**
960 **Rugnone M, Mora-García S, Yanovsky MJ, De Leone MJ, et al** (2018) The LNK Gene
961 Family: At the Crossroad between Light Signaling and the Circadian Clock. Genes (Basel)
962 **10**: 2
963 **de Leone MJ, Hernando CE, Vázquez M, Schneeberger K, Yanovsky MJ** (2020) Bacterial
964 Infection Disrupts Clock Gene Expression to Attenuate Immune Responses. Curr Biol **30**:
965 1–8
966 **Li B, Gao Z, Liu X, Sun D, Tang W** (2019) Transcriptional Profiling Reveals a Time-of-Day-
967 Specific Role of REVEILLE 4/8 in Regulating the First Wave of Heat Shock-Induced Gene
968 Expression in Arabidopsis. Plant Cell **31**: 2353–2369
969 **Li X, Liu C, Zhao Z, Ma D, Zhang J, Yang Y, Liu Y, Liu H** (2020) COR27 and COR28 are
970 Novel Regulators of the COP1-HY5 Regulatory Hub and Photomorphogenesis in
971 Arabidopsis. Plant Cell Adv Publ. doi: 10.1105/tpc.20.00195
972 **Li X, Ma D, Lu SX, Hu X, Huang R, Liang T, Xu T, Tobin EM, Liu H** (2016) Blue Light-
973 and Low Temperature-Regulated COR27 and COR28 Play Roles in the Arabidopsis
974 Circadian Clock. Plant Cell **28**: 2755–2769
975 **Ma Y, Gil S, Grasser KD, Mas P** (2018) Targeted Recruitment of the Basal Transcriptional
976 Machinery by LNK Clock Components Controls the Circadian Rhythms of Nascent RNAs
977 in Arabidopsis. Plant Cell **30**: 907–924
978 **Mikkelsen MD, Thomashow MF** (2009) A role for circadian evening elements in cold-
979 regulated gene expression in Arabidopsis. Plant J **60**: 328–339
980 **Mizuno T, Takeuchi A, Nomoto Y, Nakamichi N, Yamashino T** (2014) The LNK1 night

981 light-inducible and clock-regulated gene is induced also in response to warm-night through
982 the circadian clock nighttime repressor in Arabidopsis thaliana. Plant Signal Behav. doi:
983 10.4161/psb.28505
984 **Mockler TC, Michael TP, Priest HD, Shen R, Sullivan CM, Givan SA, Mcentee C, Kay SA,**
985 **Chory J** (2007) The diurnal project: Diurnal and circadian expression profiling, model-
986 based pattern matching, and promoter analysis. Cold Spring Harb Symp Quant Biol **72**:
987 353–363
988 **Nesvizhskii AI, Keller A, Kolker E, Aebersold R** (2003) A statistical model for identifying
989 proteins by tandem mass spectrometry. Anal Chem **75**: 4646–4658
990 **Pérez-García P, Ma Y, Yanovsky MJ, Mas P** (2015) Time-dependent sequestration of RVE8
991 by LNK proteins shapes the diurnal oscillation of anthocyanin biosynthesis. Proc Natl Acad
992 Sci U S A **112**: 5249–53
993 **Plautz JD, Kaneko M, Hall JC, Kay SA** (1997) Independent photoreceptive circadian clocks
994 throughout Drosophila. Science **278**: 1632–1635
995 **Rawat R, Takahashi N, Hsu PY, Jones MA, Schwartz J, Salemi MR, Phinney BS, Harmer**
996 **SL** (2011) REVEILLE8 and PSEUDO-REPONSE REGULATOR5 Form a Negative
997 Feedback Loop within the Arabidopsis Circadian Clock. PLoS Genet **7**: e1001350
998 **Ren X, Jiang K, Zhang F** (2020) The Multifaceted Roles of RCC1 in Tumorigenesis. Front Mol
999 Biosci **7**: 225
1000 **Romanowski A, Schlaen RG, Perez-Santangelo S, Mancini E, Yanovsky MJ** (2020) Global
1001 transcriptome analysis reveals circadian control of splicing events in Arabidopsis thaliana.
1002 Plant J **103**: 889–902
1003 **Rugnone ML, Soverna AF, Sanchez SE, Schlaen RG, Hernando CE, Seymour DK, Mancini**
1004 **E, Chernomoretz A, Weigel D, Mas P, et al** (2013) LNK genes integrate light and clock
1005 signaling networks at the core of the Arabidopsis oscillator. Proc Natl Acad Sci U S A **110**:
1006 12120–12125
1007 **Salomé PA, Clung C** (2005) What makes the Arabidopsis clock tick on time? A review on
1008 entrainment. Plant, Cell Environ **28**: 21–38
1009 **Salomé PA, Robertson Mcclung C** (2005) PSEUDO-RESPONSE REGULATOR 7 and 9 Are
1010 Partially Redundant Genes Essential for the Temperature Responsiveness of the
1011 Arabidopsis Circadian Clock. Plant Cell **17**: 791–803

1012 **Sorkin ML, Nusinow DA** (2022) Using Tandem Affinity Purification to Identify Circadian
1013 Clock Protein Complexes from Arabidopsis. *In* D Staiger, S Davis, AM Davis, eds, Plant
1014 Circadian Networks Methods Protoc. Springer US, New York, NY, pp 189–203
1015 **Thines B, Harmon FG** (2010) Ambient temperature response establishes ELF3 as a required
1016 component of the core Arabidopsis circadian clock. Proc Natl Acad Sci **107**: 3257–3262
1017 **Wang P, Cui X, Zhao C, Shi L, Zhang G, Sun F, Cao X, Yuan L, Xie Q, Xu X** (2017)
1018 *COR27* and *COR28* encode nighttime repressors integrating *Arabidopsis* circadian clock
1019 and cold response. J Integr Plant Biol **59**: 78–85
1020 **Xie Q, Wang P, Liu X, Yuan L, Wang L, Zhang C, Li Y, Xing H, Zhi L, Yue Z, et al** (2014)
1021 LNK1 and LNK2 Are Transcriptional Coactivators in the Arabidopsis Circadian Oscillator.
1022 Plant Cell **26**: 2843–2857
1023 **Zhou M, Zhang K, Sun Z, Yan M, Chen C, Zhang X, Tang Y, Wu Y** (2017) LNK1 and
1024 LNK2 Corepressors Interact with the MYB3 Transcription Factor in Phenylpropanoid
1025 Biosynthesis 1. Plant Physiol **174**: 1348–1358
1026 **Zhou Y, Park SH, Soh MY, Chua NH** (2021) Ubiquitin-specific proteases UBP12 and UBP13
1027 promote shade avoidance response by enhancing PIF7 stability. Proc Natl Acad Sci U S A.
1028 doi: 10.1073/PNAS.2103633118/SUPPL_FILE/PNAS.2103633118.SAPP.PDF
1029 **Zhu W, Zhou H, Lin F, Zhao X, Jiang Y, Xu D, Deng XW** (2020) COLD-REGULATED
1030 GENE 27 Integrates Signals from Light and the Circadian Clock to Promote Hypocotyl
1031 Growth in Arabidopsis. Plant Cell Adv Publ. doi: 10.1105/tpc.20.00192
1032
1033
1034
1035
1036
1037
1038
1039
1040
1041
1042

Table 1. Proteins coprecipitated with RVE8/LNK1/LNK2-HFC at ZT5. Total spectra for a given coprecipitated protein is shown for each independent ZT5 sample. The curated table excludes coprecipitated proteins that were identified in the GFP-HFC or Col-0 negative control APMS experiments, see Dataset S1 for all identifications.

Protein Name	AGI Locus Number	M.W. (kDa)	LNK1HFC_Z T5_1	LNK1HFC_Z T5_2	LNK2HFC_Z T5_1	LNK2HFC_Z T5_2	RVE8HFC_Z T5_1	RVE8HFC_Z T5_2
LNK1	AT5G64170‡	70	173	56	0	0	107	87
LNK2	AT3G54500‡	81	0	0	468	497	154	149
RVE8	AT3G09600‡	40	22	13	206	223	272	267
RVE6	AT5G52660	36	28	14	79	87	0	0
TCF1	AT3G55580‡	51	16	8	37	39	7	4
RVE5	AT4G01280‡	34	16	8	27	33	0	0
RCC1L	AT3G53830‡	49	4	2	8	8	0	0
RVE4	AT5G02840‡	31	4	0	85	84	0	0
CCR16	AT1G02150‡	60	1	0	0	0	0	0
RVE3	AT1G01520‡	33	0	0	10	11	0	0
GRXS17	AT4G04950	53	0	0	10	9	0	0
UBP12	AT5G06600	131	0	0	8	9	0	0
UBP13	AT3G11910	131	0	0	6	7	1	0
RACK1A	AT1G18080‡	36	0	0	2	4	0	0
DGR2	AT5G25460‡	40	0	0	4	3	1	0
PICALM3	AT5G35200‡	61	0	0	4	2	0	0
TRA1A	AT2G17930	436	0	0	0	2	0	0
CAB4	AT3G47470‡	28	0	0	1	1	0	0
BTI1	AT4G23630‡	31	0	0	1	1	0	0
PUB12	AT2G28830‡	107	0	0	0	1	0	0
ABA1	AT5G67030‡	74	0	0	0	1	0	0
FLL2	AT1G01320‡	199	0	0	1	0	0	0
WLIM1	AT1G10200‡	21	0	0	1	0	0	0
FINS1	AT1G43670‡	37	0	0	1	0	0	0
PP2A-3	AT2G42500	36	0	0	1	0	0	0
Nucleic acid-binding, OB-fold-like protein	AT3G10090	7	0	0	1	0	0	0
CPNB2	AT3G13470‡	63	0	0	0	0	31	26
LNK3	AT3G12320‡	30	0	0	0	0	24	25
SAG24	AT1G66580‡	25	0	0	0	0	4	0
LNK4	AT5G06980	32	0	0	0	0	3	3
ATRH3	AT5G26742	81	0	0	0	0	1	0

‡Indicates mRNA is circadian regulated in constant light according to analysis in Romanowski et al. (2020) The Plant Journal

1043

Table 2. Identified proteins coprecipitated with RVE8/LNK1/LNK2-HFC at ZT9. Total spectra for a given coprecipitated protein is shown for each independent ZT9 sample. The curated table excludes coprecipitated proteins that were identified in the GFP-HFC or Col-0 negative control APMS experiments, see Dataset S1 for all identifications.

Protein Name	AGI Locus Number	M.W. (kDa)	LNK1HFC_ZT9_1	LNK1HFC_ZT9_2	LNK2HFC_ZT9_1	LNK2HFC_ZT9_2	RVE8HFC_ZT9_1	RVE8HFC_ZT9_2
LNK1	AT5G64170‡	70	435	621	0	0	66	90
LNK2	AT3G54500‡	81	0	0	140	151	109	137
RVE8	AT3G09600‡	40	71	101	33	52	285	317
RVE6	AT5G52660	36	86	113	21	22	4	3
RVE5	AT4G01280‡	34	32	51	12	12	0	0
TCF1	AT3G55580‡	51	32	49	20	30	13	13
RVE4	AT5G02840‡	31	31	43	0	7	0	0
RCC1L	AT3G53830‡	49	20	25	3	10	0	0
COR28	AT4G33980‡	26	11	15	6	6	26	29
RVE3	AT1G01520‡	33	8	10	0	0	0	0
CCR16	AT1G02150‡	60	3	8	0	0	0	1
TRA1A	AT2G17930	436	3	7	0	0	0	0
DGR2	AT5G25460‡	40	3	4	0	0	2	5
ENTH/ANTH/VHS superfamily protein	AT5G35200‡	61	2	3	0	0	0	0
FLL2	AT1G01320‡	199	0	3	0	0	0	1
Nucleic acid-binding, OB-fold-like protein	AT2G40660‡	42	3	2	0	0	0	0
UBP12	AT5G06600	131	0	1	0	0	0	0
PHOT2	AT5G58140	102	1	2	0	0	0	0
MLK4	AT3G13670‡	79	0	2	0	0	6	6
UBP13	AT3G11910	131	0	2	0	0	1	4
COR27	AT5G42900	27	2	1	0	1	4	7
WLIM1	AT1G10200‡	21	1	1	0	0	1	2
CAB4	AT3G47470‡	28	1	1	0	0	1	1
MLK2	AT3G03940	78	0	0	1	1	6	7
GRXS17	AT4G04950	53	0	0	0	0	1	2
CPNB2	AT3G13470‡	63	0	0	0	0	35	41
LNK3	AT3G12320‡	31	0	0	0	0	18	23
LNK4	AT5G06980	32	0	0	0	0	2	6
COP1	AT2G32950‡	76	0	0	0	0	3	4
MLK1	AT5G18190	77	0	0	0	0	3	4
SPA1	AT2G46340‡	115	0	0	0	0	1	4
MLK3	AT2G25760	76	0	0	0	0	3	0

‡Indicates mRNA is circadian regulated in constant light according to analysis in Romanowski et al. (2020) *The Plant Journal*

Table 3. Identified proteins coprecipitated with YFP-COR27/GFP-COR28 at ZT9. Total spectra for a given coprecipitated protein is shown for each independent ZT9 sample. The curated table excludes coprecipitated proteins that were identified in the GFP-HFC or Col-0 negative control APMS experiments, see Dataset S1 for all identifications.

Protein Name	AGI Locus Number	M.W. (kDa)	YFP-COR27_ZT9_1	YFP-COR27_ZT9_2	YFP-COR27_ZT9_3	YFP-COR27_ZT9_4	GFP-COR28_ZT9_1	GFP-COR28_ZT9_2	GFP-COR28_ZT9_3	GFP_COR28_ZT9_4
COR27	AT5G42900	27	89	85	95	80	0	0	0	0
COR28	AT4G33980‡	26	0	0	0	0	22	18	8	10
COP1	AT2G32950‡	76	16	12	19	16	6	6	1	2
SPA1	AT2G46340‡	115	16	12	16	13	4	6	1	0
MLK4	AT3G13670‡	79	16	11	15	12	0	0	0	0
MLK2	AT3G03940	78	13	12	15	12	0	0	0	0
PHYD	AT4G16250	129	8	7	13	11	0	0	0	0
MLK1	AT5G18190	77	10	10	12	10	0	0	0	0
SPA4	AT1G53090	89	8	4	11	7	0	0	0	0
SPA2	AT4G11110	115	8	6	10	6	0	1	0	0
SF1	AT5G51300	87	7	12	7	5	0	0	0	0
RVE8	AT3G09600‡	40	7	5	7	6	3	4	0	3
LNK2	AT3G54500‡	81	6	5	6	3	0	1	0	0
MLK3	AT2G25760	76	5	6	6	8	0	0	0	0
LNK1	AT5G64170‡	70	4	4	5	4	4	3	1	0
SPA3	AT3G15354‡	93	4	4	4	4	0	0	0	0
RVE6	AT5G52660	36	3	3	4	1	1	0	0	0
RVE5	AT4G01280‡	34	1	1	2	0	1	0	0	0
CCR2	AT2G21660‡	17	1	0	1	1	0	0	0	0
TCF1	AT3G55580‡	51	0	0	1	0	0	0	0	0
PHYE	AT4G18130‡	123	1	0	0	0	0	0	0	0

‡Indicates mRNA is circadian regulated in constant light according to analysis in Romanowski et al. (2020) The Plant Journal

1045

1046

1047